

Quantum Causal Unravelling

Ge Bai,^{1,2} Ya-Dong Wu,^{1,2} Yan Zhu,^{1,2} Masahito Hayashi,^{3,4,5} and Giulio Chiribella^{1,6,2,7,*}

¹*QICI Quantum Information and Computation Initiative, Department of Computer Science,
The University of Hong Kong, Pokfulam Road, Hong Kong*

²*HKU-Oxford Joint Laboratory for Quantum Information and Computation*

³*Shenzhen Institute for Quantum Science and Engineering,
Southern University of Science and Technology, Shenzhen 518055, China*

⁴*Guangdong Provincial Key Laboratory of Quantum Science and Engineering,
Southern University of Science and Technology, Shenzhen 518055, China*

⁵*Graduate School of Mathematics, Nagoya University, Nagoya, 464-8602, Japan*

⁶*Department of Computer Science, University of Oxford, Parks Road, Oxford OX1 3QD, United Kingdom*

⁷*Perimeter Institute For Theoretical Physics, 31 Caroline Street North, Waterloo N2L 2Y5, Ontario, Canada*

Complex processes often arise from sequences of simpler interactions involving a few particles at a time. These interactions, however, may not be directly accessible to experiments. Here we develop the first efficient method for unravelling the causal structure of the interactions in a multipartite quantum process, under the assumption that the process has bounded information loss and induces causal dependencies whose strength is above a fixed (but otherwise arbitrary) threshold. Our method is based on a quantum algorithm whose complexity scales polynomially in the total number of input/output systems, in the dimension of the systems involved in each interaction, and in the inverse of the chosen threshold for the strength of the causal dependencies. Under additional assumptions, we also provide a second algorithm that has lower complexity and requires only local state preparation and local measurements. Our algorithms can be used to identify processes that can be characterized efficiently with the technique of quantum process tomography. Similarly, they can be used to identify useful communication channels in quantum networks, and to test the internal structure of uncharacterized quantum circuits.

I. Introduction

Many processes in nature arise from sequences of basic interactions, each involving a small number of physical systems. Determining the causal structure of these interactions is important both for basic science and for engineering. Often, however, the sequence of interactions giving rise to a process of interest may not be directly accessible to experiments. For example, scattering experiments in high energy physics can probe the relation between a set of incoming particles and a set of outgoing particles, but typically cannot access the individual events taking place

* giulio@cs.hku.hk

within the scattering region. In this and similar scenarios, a fundamental problem is to characterize the causal structure of the interactions by accessing only the inputs and outputs of the process of interest, while treating the intermediate steps as a black box. We call this problem, illustrated in [Figure 1](#), the causal unravelling of an unknown physical process. Explicitly, the problem of causal unravelling is to determine whether an unknown process can be broken down into a sequence of simpler interactions, to determine the order of such interactions, and to determine which systems take part in each interaction. Causal unravelling can be viewed as a special case of the broader problem of causal discovery [[1](#), [2](#)], namely the task to identify the causal relations between a given set of variables. In the broad class of causal discovery problems, the distinctive features of causal unraveling are that (i) the goal is to identify a linear causal structure, corresponding to the sequence of interactions underlying the given process, and (ii) certain variables are *a priori* known to be ‘inputs’ (and therefore potential ‘causes’), while other variables are *a priori* known to be ‘outputs’ (and therefore potential ‘effects’). This scenario often arises in experimental physics, where the input/output structure is typically clear from the design of the experiment, as in the aforementioned example of scattering experiments. In principle, candidate answers can be extracted from a full tomographic characterization of the process under consideration. However, the complexity of process tomography grows exponentially in the number of inputs and outputs, making this approach unfeasible when the process involves a large number of systems.

In the classical domain, the problem of causal unravelling can be efficiently addressed with a variety of algorithms developed for the general problem of causal discovery [[1–3](#)]. Classical causal discovery algorithms often formulate causal relationships with graphical models and solve such models by structure learning algorithms, such as PC algorithm (named after Peter Spirtes and Clark Glymour) [[1](#)], Greedy Equivalence Search [[4](#)], and Max-Min Hill Climbing [[5](#)]. These algorithms cover a wide variety of problems, by making different sets of assumptions on the process under consideration. Typical assumptions include causal sufficiency—meaning that no variables are hidden—and causal faithfulness—meaning that the conditional independences among the variables are precisely those associated to an underlying graph used to model the causal structure. In general, however, causal discovery is intrinsically a hard problem: when no assumption is made, the complexity of all the known algorithms becomes exponential in the worst case over all possible instances [[6](#), [7](#)].

In the quantum domain, the problem of causal unravelling is made even more challenging by the presence of correlations that elude a classical explanation [[8](#), [9](#)]. In recent years, the quantum extension of the notion of causal model has been addressed in a series of works [[10–15](#)], providing a solid conceptual foundation to the field of quantum causal discovery. On the algorithmic side, however, the study of quantum causal models remained relatively underdeveloped. Specific instances of quantum causal discovery were studied in Refs. [[16–18](#)], showing that quantum resources offer appealing advantages. These examples, however, were limited to simple instances, typically involving a small number of variables and/or a small number of hypotheses on the causal structure. In more general scenarios, one approach could be to perform quantum process tomography and then to infer the causal structure from the full description of the process under consideration [[19](#)]. As in the classical case, however, the number of queries needed by a full process tomography grows exponentially with the number of systems involved in the process, making this approach

impractical as the size of the problem increases.

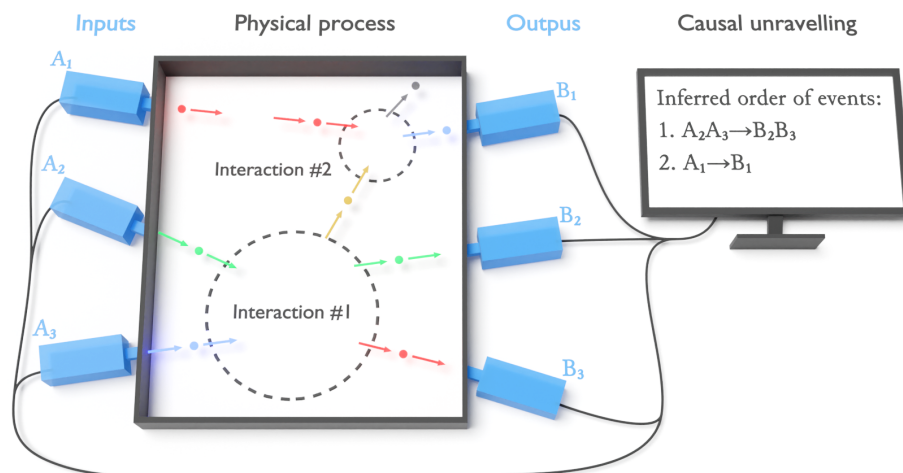


FIG. 1. **Causal unravelling.** A physical process involves a set of input systems (in the figure, A_1 , A_2 , and A_3) and a set of output systems (in the figure, B_1 , B_2 , and B_3). The process is the result of a sequence of interactions, each of which involves a subset of the inputs and a subset of the outputs. The problem is to infer the causal structure of the interactions solely from the input-output behaviour of the process.

In this paper, we provide an efficient algorithm for unravelling the causal structure of multipartite quantum processes without resorting to full process tomography. Our algorithm is similar to the PC algorithm [1] for classical causal discovery, in that it is based on a set of tests that establish the independence relations between subsets of input and output systems. We show that the algorithm has the following features:

1. The number of independence tests needed to infer the causal structure scales polynomially with the number of inputs/outputs of the process. This feature is possible thanks to the special structure of the causal unravelling problem, where the goal is to establish a linear ordering of the interactions giving rise to the process under consideration.
2. The independence tests produce, as a byproduct, an estimate of the strength of correlation between the various inputs and outputs of the process. In Methods, we show that this estimate can be obtained by performing a number of measurements that grows polynomially with the dimension of the systems under consideration, and that the number of measurements needed to conclude independence scales polynomially with the number of systems.
3. The algorithm is exact whenever the process has bounded information loss, and satisfies a form of causal faithfulness property, namely that the strength of the causal relations, when present, is above a given threshold. When these assumptions are not satisfied, the algorithm produces an approximate result. The details of the approximate case are in [Supplementary Note 6](#).

Moreover, the efficiency of our algorithm can be further boosted in special cases, including (i) the case where each input of a given interaction has a non-trivial causal influence on all the outputs of subsequent interactions, and (ii)

the case where the process belongs to a special case of Markovian processes [12, 19–21], where each output depends only on one previous input and each input affects only one later output. We study these cases in the Results, where we devise an alternative algorithm that only requires local state preparations and local measurements. The number of queries to the process is only logarithmic in the number of input and output wires, thanks to a method that efficiently determines the correlations between input-output pairs as described in the Methods.

The remaining parts of this paper is structured as follows. In Results, we first formulate the quantum causal unravelling problem. In the second subsection, we give the main body of the efficient causal unravelling algorithm, discuss the assumptions and analyze its efficiency. The third subsection of Results talks about the alternative algorithm designed for special cases. At the end of Results, we briefly talk about a generalization of our algorithm. Future works, interpretations and the applications of the causal unravelling algorithms are addressed in the Discussion. The Methods section contains the detailed implementation of the independence tests used by the algorithms in Results.

II. Results

Problem formulation. Let us start by giving a precise formulation of the problem of quantum causal unravelling. In this problem, an experimenter is given access to a multipartite quantum process, with inputs labelled as $A_1, \dots, A_{n_{\text{in}}}$, and outputs labelled as $B_1, \dots, B_{n_{\text{out}}}$. Note that, in general, different labels may refer to the same physical system: for example, system A_1 could be a single photon with a given frequency, entering in the interaction region, and system B_1 could be a single photon with the same frequency, exiting the interaction region. Mathematically, the process is described by a quantum channel, that is, a completely positive trace-preserving (CPTP) linear map \mathcal{C} transforming operators on the tensor product space $\mathcal{H}_{A_1} \otimes \dots \otimes \mathcal{H}_{A_{n_{\text{in}}}}$ to operators on the tensor product space $\mathcal{H}_{B_1} \otimes \dots \otimes \mathcal{H}_{B_{n_{\text{out}}}}$. Note that, without loss of generality, one can always assume $n_{\text{in}} = n_{\text{out}} = n$, as this condition can be satisfied by adding a number of dummy systems with one-dimensional Hilbert space. In the following, we will denote by $L(\mathcal{H})$ the set of linear operators on a generic Hilbert space \mathcal{H} , and by $S(\mathcal{H})$ the subset of density operators on \mathcal{H} , that is, the subset of operators $\rho \in L(\mathcal{H})$ that are positive semidefinite and have unit trace.

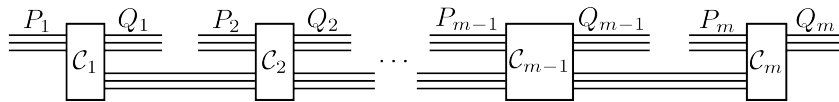


FIG. 2. **Decomposition of a physical process into a sequence of m interactions.** The inputs (outputs) of the processes are divided into m non-overlapping subsets. The i -th subset of the inputs (outputs) consists of the systems that enter (exit) the interaction at the i -th step (rectangular boxes in the picture). The wires connecting one interaction to the next represent intermediate systems that in this stage are not directly accessible to experiments. For example, a photon could enter the first interaction, remain as an intermediate system between the first and second interaction, and then exit the interaction region after the second interaction.

The problem of causal unravelling is to determine whether a multipartite process can be broken down into a sequence of interactions, as in Figure 2, and, in the affirmative case, to determine which systems are involved in each interaction. Mathematically, the problem is to find a partition $\{P_i\}_{i=1}^m$ of the set $\{A_1, \dots, A_n\}$ and a partition $\{Q_i\}_{i=1}^m$

of the set $\{B_1, \dots, B_n\}$, such that the multipartite process can be decomposed into a sequence of interactions, with the i -th interaction involving input systems in P_i and output systems in Q_i . Such a sequential structure matches the framework of quantum combs [22, 23]. A quantum comb is a quantum process that can be broken down into a sequence of interactions $\mathcal{C}_1, \dots, \mathcal{C}_k$ as in Figure 2, while each interaction \mathcal{C}_i is a CPTP map and is called a tooth of the comb. Refs. [22, 23] give a set of necessary and sufficient conditions for determining whether a given process conforms to a quantum comb, which is equivalent to whether the process admits a causal unravelling with partitions $\{P_i\}$ and $\{Q_i\}$. We say a process \mathcal{C} has a causal unravelling $(P_1, Q_1), \dots, (P_m, Q_m)$ if it can be decomposed into the form of a quantum comb with m teeth as in Figure 2.

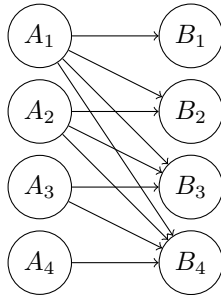


FIG. 3. **Causal graph of a quantum process with causal unravelling** $(A_1, B_1), (A_2, B_2), (A_3, B_3), (A_4, B_4)$. This is a bipartite graph because inputs can be independently controlled, and every two outputs are independent conditioned on all inputs.

The causal unravelling of a given multipartite process determines the possible signalling relations between inputs and outputs. With respect to this decomposition, input systems at a given time can only signal to output systems at later times. The resulting pattern can be graphically illustrated by a causal graph [1, 2, 14], as shown in Figure 3. Note that the causal graph includes all the signalling relations that are in principle compatible with the structure of the interactions. However, a specific quantum process may not exhibit any signalling from a specific input to a specific output, even though the causal structure of the interactions would in principle permit it. When this occurs, the causal unravelling of a process may not be unique. For example, consider a bipartite process with inputs $\{A_1, A_2\}$ and outputs $\{B_1, B_2\}$, with the property that A_1 signals to B_1 but not to B_2 and A_2 signals to B_2 but not to B_1 . It is impossible to decide whether the signalling $A_1 \rightarrow B_1$ happens before or after $A_2 \rightarrow B_2$ since they are causally uncorrelated. Therefore, the process admits two causal unravellings: $(A_1, B_1), (A_2, B_2)$ and $(A_2, B_2), (A_1, B_1)$. In this case, any of the two options is a valid solution of the causal unravelling problem.

Generally, causal discovery is a hard problem, even in the classical setting [6, 7]. However, we will now show that, under a few assumptions, the more specific problem of quantum causal unravelling defined above can be solved efficiently. The first assumption is that the basic interactions appearing in the causal unravelling involve a small number of systems, independent of the number of inputs and outputs. At the fundamental level, this assumption is motivated by the fact that interactions are local, and typically involve a small number of systems. Mathematically, the assumption is that the cardinality of all the sets in the partitions $\{P_i\}_{i=1}^m$ and $\{Q_i\}_{i=1}^m$ is no larger than a constant

c independent of n . For simplicity, we will first restrict our attention to the special case $c = 1$, meaning that the process can be broken down into interactions involving only one input and one output at a time. We will discuss larger c at the end of the Results and in [Supplementary Note 7](#). Hereafter, we will denote by $\text{Comb}[(A_1, B_1), \dots, (A_n, B_n)]$ the set of quantum combs with n teeth where the i -th tooth has input A_i and output B_i .

In the basic $c = 1$ scenario illustrated above, the problem of causal unravelling is to find out which pair of systems is involved in the first interaction, which pair is involved in the second, and so on. Formally, our goal is to identify an ordering of the inputs and outputs, $(A_{\sigma(1)}, B_{\pi(1)}), \dots, (A_{\sigma(n)}, B_{\pi(n)})$ with σ and π being permutations of $\{1, \dots, n\}$, such that $\mathcal{C} \in \text{Comb}[(A_{\sigma(1)}, B_{\pi(1)}), \dots, (A_{\sigma(n)}, B_{\pi(n)})]$.

To quantify the efficiency of our algorithms, we will focus on the sample complexity, namely the number of black-box queries to the channel \mathcal{C} , and on the computational complexity, including additional quantum and classical computation time measured by the number of elementary quantum gates and classical operations.

Efficient quantum causal unravelling. We now provide an efficient quantum algorithm for quantum causal unravelling. The main idea of the algorithm is to recursively find the last interaction in the decomposition of a given process. To illustrate this idea, consider the example of [Figure 3](#). When we remove B_4 , the node A_4 becomes disconnected from all the other nodes, meaning that the state of system A_4 does not affect the state of the other systems. By testing this independence condition, we can in principle check whether the graph of [Figure 3](#) is an appropriate model for the process under consideration. In general, suppose (A_x, B_y) are the input and output of the last interaction. Since A_x signals to only B_y , if we ignore B_y , A_x is independent of the joint system formed by all systems excluding A_x and B_y . This gives the following criterion that the last interaction must satisfy:

Proposition 1. [\[22\]](#) *The last interaction of a process \mathcal{C} involves the input/output pair (A_x, B_y) if and only if A_x is independent of $A_{\neq x}B_{\neq y}$, the joint system containing all systems other than A_x and B_y .*

More details can be found in [Supplementary Note 1](#). By scanning the possible pairs (A_x, B_y) , we can find if one of them satisfy the above criterion, and in the affirmative case, we can assign that pair to the last interaction. Note that, in general, there may be more than one pair that satisfy the required condition. After one pair is found, one can reduce the problem to a smaller graph containing $n - 1$ inputs and $n - 1$ outputs. If at every step a suitable pair is found, then the final result is a valid causal unravelling of the original process. If at one step no pair can be found, the algorithm will then conclude that no causal unravelling with $c = 1$ exists for the remaining subgraph. At this point, the algorithm can continue by considering causal unravellings with higher values of c for the remaining subgraph, which is discussed at the end of the Results and detailed in [Supplementary Note 7](#).

A description of the algorithm is provided in [Algorithm 1](#). The algorithm runs in a recursive manner: for an n -tooth comb, it finds the last tooth of the comb, remove the tooth (feeds the input with an arbitrary state and discards its output), and reduces the problem to finding the causal unravelling of an $(n - 1)$ -tooth comb. We repeat the above procedure until we reach the bottom case $n = 1$, and thus obtain the order of all inputs and outputs. If the last tooth cannot be found in some iteration, it means that the current channel cannot be further decomposed, and the

algorithm will output the trivial causal unravelling (P, Q) where P (Q) is the set of all input (output) wires of the current channel.

Algorithm 1: Efficient quantum causal unravelling algorithm

```

Input : Black-box access to quantum channel  $\mathcal{C}$ 

Output : A causal unravelling of  $\mathcal{C}$ 

1  if  $\mathcal{C}$  has only one input wire  $A_x$  and one output wire  $B_y$  then
2  |   Output  $(A_x, B_y)$  and exit;
3  end

4  foreach input-output pair  $(A_x, B_y)$  of  $\mathcal{C}$  do
5  |   if  $(A_x, B_y)$  is the last tooth then // Done by checking whether  $A_x$  and  $A_{\neq x} B_{\neq y}$  are independent
6  |   |   using the quantum circuit described in the Methods
7  |   |   Let  $\mathcal{C}_{A_{\neq x}, B_{\neq y}}(\rho) := \text{Tr}_{B_y}[\mathcal{C}(\rho \otimes \tau_{A_x})]$ , where  $\tau_{A_x}$  is an arbitrary state on system  $A_x$ ;
8  |   |   |   // Remove  $A_x$  and  $B_y$  from  $\mathcal{C}$ 
9  |   |   Recursively run this algorithm on the reduced channel  $\mathcal{C}_{A_{\neq x}, B_{\neq y}}$ ;
10 |   |   Output  $(A_x, B_y)$  and exit; // Append  $(A_x, B_y)$  to the end of the output
11 |   end
12 end

13 Let  $P$  ( $Q$ ) be the set of all input (output) wires of  $\mathcal{C}$ ;
14 Output  $(P, Q)$  and exit; // Cannot be further decomposed

```

We now discuss the efficiency of this algorithm. First, we show that the number of independence tests is polynomial in n . Let $T_{\text{test}}(n)$ be the number of independence tests required for an n -to- n channel. In this algorithm, an independence test is performed for at most each of the n^2 input-output pairs (A_x, B_y) , resulting in $O(n^2)$ independence tests. After finding a last tooth, the problem size is reduced to $n - 1$. Therefore, $T_{\text{test}}(n)$ can be given by the recursive relation $T_{\text{test}}(n) = O(n^2) + T_{\text{test}}(n - 1)$ with $T_{\text{test}}(1) = O(1)$, solving which gives $T_{\text{test}}(n) = O(n^3)$.

Second, we show that the independence tests can be efficiently realized. This is a non-trivial problem, because testing whether two generic systems are in a product state is computationally hard in the worst-case scenario [24]. Nevertheless, in the Methods we design a quantum circuit that performs the independence tests efficiently under assumptions of bounded information loss and causal faithfulness. Our circuit converts the independence test to the estimation of the distance between quantum states, which is done by the SWAP test [25].

Now, we give the efficiency guarantee for our algorithm. We first discuss the exact case, when our algorithm produces the exact causal unravelling of \mathcal{C} based on two assumptions. We will use a few parameters related to the Choi state [26] of the process \mathcal{C} , defined as the state $C := (\mathcal{C} \otimes \mathcal{I})(|I\rangle\rangle \langle\langle I|)/d_{\text{in}}$, where d_{in} is the total dimension of all the input systems, and $|I\rangle\rangle = \sum_{j=1}^{d_{\text{in}}} |j\rangle \otimes |j\rangle$ is the canonical (unnormalized) maximally entangled state. The rank of the Choi state C is called the Kraus rank of the process \mathcal{C} . Since a unitary evolution, namely a process without information loss, has Kraus rank equal to one, the Kraus rank could be interpreted as the degree of information loss

introduced by the process.

An important parameter entering into the analysis is the degree of independence between systems, defined in the following. For a state ρ , we say two disjoint subsystems S and T are independent if $\rho_{ST} = \rho_S \otimes \rho_T$, where ρ_S , ρ_T and ρ_{ST} are the marginal states of ρ on the subsystems S , T and the joint system ST , respectively. The degree of independence between S and T is then defined as $\chi_1(S; T)_\rho := \|\rho_{ST} - \rho_S \otimes \rho_T\|_1$, where $\|X\|_1 := \text{Tr}[\sqrt{X^\dagger X}]$ denotes the trace norm. Clearly, $\chi_1(S; T)_\rho = 0$ if and only if $\rho_{ST} = \rho_S \otimes \rho_T$. More generally, the trace distance is related to the probability to distinguish the states, and thus $\chi_1(S; T)_\rho$ measures the probability that an observer correctly decides whether the subsystems are independent or correlated. In the following, we will apply this definition to the Choi state C of the process \mathcal{C} . With this choice, $\chi_1(S; T)_C$ satisfies the conditions for a quantum causality measure, as defined in Ref. [27].

To facilitate the efficiency analysis of our algorithm, we first put the process \mathcal{C} in a standard form where all input and output wires have the same dimension d_A . This standard form does not limit the generality of the quantum process we investigate. For a process \mathcal{C} with input dimensions d_{A_1}, \dots, d_{A_n} and output dimensions d_{B_1}, \dots, d_{B_n} , we can pick $d_A = \max\{d_{A_1}, \dots, d_{A_n}, d_{B_1}, \dots, d_{B_n}\}$ and regard each input or output wire of \mathcal{C} as a subspace of a d_A -dimensional system, thus transforming \mathcal{C} into a process whose wires all have dimension d_A . In our analysis, we will use the Kraus rank of the process in the standard form to characterize the information loss. We assume that the information loss is bounded, which is given by the following assumption:

Assumption 1. *The Kraus rank of \mathcal{C} , after transforming it into the standard form, is bounded by a polynomial of n .*

To ensure that the algorithm outputs the correct causal unravelling, we further require that the process satisfies a form of causal faithfulness, meaning that the strength of causal relations is either zero or above a threshold. Using χ_1 as a quantitative measure of correlation, we adopt the following assumption:

Assumption 2. *There exists a number $\chi_{\min} > 0$ such that, for any two disjoint sets of wires S and T being tested for independence, either*

1. $\chi_1(S; T)_C = 0$, or
2. $\chi_1(S; T)_C \geq \chi_{\min}$,

where C is the Choi state of the quantum process \mathcal{C} .

The threshold χ_{\min} determines the resolution of the independence tests. To guarantee the correctness of [Algorithm 1](#), the independence tests must be precise enough to detect correlations above this threshold with high probability. The efficiency and correctness of [Algorithm 1](#) are given in the following theorem, whose proof is in [Supplementary Note 2](#):

Theorem 1. *Under Assumptions 1 and 2, for any confidence parameter $\kappa_0 > 0$, [Algorithm 1](#) satisfies the following conditions:*

1. *With probability $1 - \kappa_0$, the output of [Algorithm 1](#) is a correct causal unravelling for \mathcal{C} .*

2. The number of queries to \mathcal{C} is in the order of

$$T_{\text{sample}} = O(n^3 d_A^2 r_{\mathcal{C}}^2 \chi_{\min}^{-4} \log(n \kappa_0^{-1})) \quad (1)$$

where $r_{\mathcal{C}}$ is the Kraus rank of \mathcal{C} in the standard form with all wires having dimension d_A .

3. The computational complexity is in the order of $O(T_{\text{sample}} n \log d_A)$.

Theorem 1 guarantees that, under appropriate assumptions, the sample complexity of our algorithm is polynomial in the number of input and output systems of the process under consideration. This feature is in stark contrast with the exponential complexity of full process tomography. As a consequence, our algorithm offers a speedup over for other algorithms, such as the one proposed in Ref. [19], which require process tomography as an intermediate step.

Assumptions 1 and 2 guarantee that **Algorithm 1** produces an exact causal unravelling. However, both assumptions can be lifted if we only require an approximate causal unravelling, meaning that the process \mathcal{C} is within a certain error of another process compatible with the causal unravelling output by the algorithm. In **Supplementary Note 6**, we formulate this approximate case and prove that the error is small under the condition that every marginal Choi state of \mathcal{C} obtained by taking only the first k inputs and $k - 1$ outputs in the causal unravelling of \mathcal{C} has polynomial rank up to a small error. This condition can be verified efficiently during the execution of **Algorithm 1**.

Causal unravelling with local observations. We now show that, under some assumptions on the input-output relations, one can design algorithms that have much lower sample complexity in terms of n compared to **Algorithm 1**, and are more experimentally friendly, in that they require only local state preparation and local measurements.

In the Methods, we show an efficient algorithm to detect the pairwise correlations between input and output wires of \mathcal{C} with local state preparation and local measurements. The algorithm computes a Boolean matrix ind_{ij} such that, with high probability, for every i and j , A_i and B_j are approximately independent whenever $\text{ind}_{ij} = \text{true}$, and are correlated whenever $\text{ind}_{ij} = \text{false}$. With some assumptions, this Boolean matrix ind_{ij} is sufficient to give the exact causal unravelling. The first case is given by the following assumption on the process \mathcal{C} :

Assumption 3. \mathcal{C} is a quantum comb in $\text{Comb}[(A_{\sigma(1)}, B_{\pi(1)}), \dots, (A_{\sigma(n)}, B_{\pi(n)})]$, and there exists a constant $\chi_{\min} > 0$ such that, for any pair of input and output wires $A_{\sigma(i)}$ and $B_{\pi(j)}$, if $j \geq i$, then $\chi_1(A_{\sigma(i)}; B_{\pi(j)})_{\mathcal{C}} \geq \chi_{\min}$.

Assumption 3 indicates a non-trivial correlation between any pair consisting of an input system and an output system, with the property that the input system appears before the output system in the overall causal order. In other words, for any $j \geq i$, $C_{A_{\sigma(i)}, B_{\pi(j)}}$ is away from $C_{A_{\sigma(i)}} \otimes C_{B_{\pi(j)}}$ by distance χ_{\min} . Meanwhile, **Assumption 3** defines a total order of the input (output) wires, and ensures a unique causal unravelling that \mathcal{C} is compatible with. Under this assumption, if A_i is the k -th input, namely $i = \sigma(k)$, A_i is correlated with $n - k + 1$ output wires including every output $B_{\pi(j)}$ with $j \geq k$, and is independent of the other outputs. In other words, if we find A_i is correlated with exactly $c_A(i)$ output wires, it must be the $(n - c_A(i) + 1)$ -th input. With this, the order of input wires can be exactly determined, and a similar statement can be applied to order the output wires.

In [Supplementary Note 4](#), we give the details of this algorithm, and analyze its efficiency given by the following theorem:

Theorem 2. *For a quantum comb $\mathcal{C} \in \text{Comb}[(A_{\sigma(1)}, B_{\pi(1)}), \dots, (A_{\sigma(n)}, B_{\pi(n)})]$ satisfying [Assumption 3](#), there is an algorithm that satisfies the following conditions:*

1. *With probability $1 - \kappa$, the algorithm outputs the correct causal unravelling $(A_{\sigma(1)}, B_{\pi(1)}), \dots, (A_{\sigma(n)}, B_{\pi(n)})$.*
2. *The algorithm uses only local state preparations and local measurements and the number of queries to \mathcal{C} is in the order of*

$$N = O(d_A^6 d_B^6 \chi_{\min}^{-2} \log(nd_A d_B \kappa^{-1})), \quad (2)$$

where $d_A := \max_i d_{A_i}$, $d_B := \max_j d_{B_j}$.

3. *The computational complexity is in the order of $O(Nn(n + d_A + d_B^4))$.*

Note the sample complexity of this algorithm grows only logarithmically with n .

A similar idea could be adopted to the case where the process belongs to a special case of Markovian processes [\[12, 19–21\]](#), where each output depends only on one previous input and each input affects only one later output. This indicates that the process is decomposable to a tensor product of n channels each with one input and one output. In our problem, the order of inputs and outputs is unknown, and we have the following assumption:

Assumption 4. *The process \mathcal{C} is a tensor product of n channels, $\mathcal{C} = \bigotimes_{i=1}^n \mathcal{C}_i$ with $\mathcal{C}_i : \mathcal{H}_{A_i} \rightarrow \mathcal{H}_{B_{\pi'(i)}}$ for some permutation π' .*

Since each output is related to at most one input and each input affects at most one output, after obtaining ind_{ij} , we can obtain the causal unravelling by matching each input-output pair (A_i, B_j) with $\text{ind}_{ij} = \mathbf{false}$.

If there exists a threshold $\chi_{\min} > 0$ such that either $\chi_1(A_i; B_j)_C = 0$ or $\chi_1(A_i; B_j)_C \geq \chi_{\min}$ holds for every A_i and B_j , then the algorithm has the same complexity as in [Theorem 2](#) that is logarithmic in n . However, in case a threshold χ_{\min} is not known, we can still show that the algorithm is efficient yet produces an approximate answer with an error bound defined by the diamond norm [\[28\]](#). The diamond norm, also known as the completely bounded trace norm, is a distance measure between channels defined for $\mathcal{C}, \mathcal{D} : L(\mathcal{H}_A) \rightarrow L(\mathcal{H}_B)$ as $\|\mathcal{C} - \mathcal{D}\|_{\diamond} := \max_{\rho \in S(\mathcal{H}_A \otimes \mathcal{H}_A)} \|(\mathcal{C} \otimes \mathcal{I}_A)(\rho) - (\mathcal{D} \otimes \mathcal{I}_A)(\rho)\|_1$, where $\mathcal{I}_A : L(\mathcal{H}_A) \rightarrow L(\mathcal{H}_A)$ is the identity map. The diamond norm measures the maximum probability to distinguish two channels, and is tighter than the trace distance since $\|\mathcal{C} - \mathcal{D}\|_{\diamond} \leq \|\mathcal{C} - \mathcal{D}\|_1$ for all channels \mathcal{C} and \mathcal{D} with Choi states C and D . The error bound is stated in the following theorem, whose proof is in [Supplementary Note 5](#).

Theorem 3. *For a quantum process \mathcal{C} satisfying [Assumption 4](#), there is an algorithm that outputs a causal unravelling $(A_1, B_{\pi(1)}), \dots, (A_n, B_{\pi(n)})$ satisfying the following conditions:*

1. With probability $1 - \kappa$, the causal unravelling is approximately correct in the following sense:

$$\exists \mathcal{D} \in \text{Comb}[(A_1, B_{\pi(1)}), \dots, (A_n, B_{\pi(n)})], \|\mathcal{C} - \mathcal{D}\|_{\diamond} \leq \varepsilon. \quad (3)$$

2. The algorithm uses only local state preparations and local measurements and the number of queries to \mathcal{C} is in the order of

$$N = O(n^2 d_A^8 d_B^6 \varepsilon^{-2} \log(nd_A d_B \kappa^{-1})), \quad (4)$$

where $d_A := \max_i d_{A_i}$ and $d_B := \max_j d_{B_j}$.

3. The computational complexity is in the order of $O(Nn(n + d_A + d_B^4))$.

Causal unravelling with interactions between more inputs and outputs. In the algorithms shown so far, we assumed that the process under consideration admits a causal unravelling where each interaction involves exactly one input and one output. More generally, [Algorithm 1](#) can be easily extended to the scenario where each interaction involves at most c inputs and c outputs of the original process. Instead of considering each wire separately, the idea is to consider a subset of at most c input (output) wires and perform independence tests on the subsets.

In [Algorithm 1](#), one enumerates an input-output pair (A_x, B_y) and checks whether it is the last tooth by performing an independence test between A_x and $A_{\neq x} B_{\neq y}$. To deal with larger c , we replace this procedure by enumerating a subset of input wires $P \subset \{A_1, \dots, A_{n_{\text{in}}}\}$ and a subset of output wires $Q \subset \{B_1, \dots, B_{n_{\text{out}}}\}$, satisfying $|P| \leq c$ and $|Q| \leq c$. Then we check whether (P, Q) is the last tooth of \mathcal{C} , which, according to [Proposition 1](#), is equivalent to checking the independence between P and $A_{\notin P} B_{\notin Q} := \{A_i | A_i \notin P\} \cup \{B_j | B_j \notin Q\}$. The independence tests can still be implemented with SWAP tests. Like [Algorithm 1](#), after we decide (P, Q) to be the last tooth, the wires in P and Q are removed from consideration, and the problem is reduced to the causal unravelling of a smaller channel. This process is done recursively until one reaches the bottom case. We give the detailed algorithm and analysis in [Supplementary Note 7](#). For constant c , under some assumptions, the complexity of the algorithm is still polynomial in n and d_A , while the exponent depends on c .

III. Discussion

In this paper we developed an efficient algorithm for discovering linear causal structures between the inputs and outputs of a multipartite quantum process. Our algorithm provides a partial solution to the more general quantum causal discovery problem, whose goal is to produce a full causal graph describing arbitrary causal correlations in an arbitrary set of quantum variables. Our algorithm can be used as the first step for quantum causal discovery, and to obtain the full causal structure, additional tests may be adopted to detect signalling between more subsets of input and output wires. Since the most general quantum causal discovery problem is intrinsically hard, an interesting

direction for future work is to examine to what extent the problem of quantum causal discovery can be solved by an efficient algorithm in scenarios beyond the linear structure analyzed in this work.

The efficiency of our algorithms relies on some assumptions. For [Algorithm 1](#), the low-rank assumption is the key in both the exact case ([Assumption 1](#)) and the approximate case discussed in [Supplementary Note 6](#). This assumption avoids the computational difficulty of deciding whether a completely general state is a product state [\[24\]](#). Physically, a quantum process has a low rank if the number of uncontrolled particles entering and/or exiting the interaction region is small. In this picture, the uncontrolled particles in the input can be regarded as sources of environmental noise, and the uncontrolled particles in the output are responsible for information loss in the process. Intuitively, without the low-rank assumption, the causal correlations will be obscured by the noise, and it will be hard to discover them without additional prior knowledge. On the other hand, if one has prior knowledge, as in the case of processes satisfying [Assumptions 3](#) and [4](#), the low-rank assumption may be lifted.

The ability to infer the underlying causal structure of a process is useful for a variety of applications. Classically, discovering causal relationships is the goal of many research areas with numerous applications in social and biomedical sciences [\[1\]](#) such as the construction of the gene expression network [\[29\]](#). Causal discovery allows us to understand complex systems whose internal structures are not directly accessible, and to discover possible models for the internal mechanisms. Quantum causal discovery, likewise, enables the modelling of quantum physical processes with inaccessible internal structure, for example, discovering the individual interactions in scattering experiments. Below we list some specific examples where our causal unravelling algorithms can be applied to the detection of correlations and the modelling of internal structures of complex processes.

First, causal relations among quantum variables are relevant to the study of quantum networks [\[30–32\]](#), where the presence of a causal relation between two systems can be used to test whether it is possible to send signals from one node to another. In a realistic setting, the signalling patterns within a quantum network may change dynamically, depending on the number of users of the network at a given moment of time, on the way the messages are routed from the senders to the receivers, and also on changes in the environment, which may affect the availability of transmission paths between nodes. Such a dynamical structure occurs frequently in classical wireless networks [\[33, 34\]](#), and is likely to arise in a future quantum internet. In this context, our algorithms provide an efficient way to detect dynamical changes in the availability of data transmission paths.

The detection of causal relations is also relevant to the verification of quantum devices, as it can be used as an initial test to determine whether a given quantum device generates input-output correlations with a desired causal structure. Such a test could serve as an initial screening to rule out devices that are not suitable for a given task, and could be followed by more refined quantum benchmarks [\[35\]](#) which quantify how well the device performs a desired task. In this context, the benefit of the causal unravelling test is that it could save the effort of performing more refined tests in case the process under consideration does not comply with the desired causal structure.

Finally, our causal unravelling algorithm can be used as a preliminary step to full process tomography. By detecting the causal structure of multipartite quantum processes, one can sometimes design a tailor-made tomography scheme

that ignores unnecessary correlations, and achieves full process tomography without requiring an exponentially large number of measurement setups. For example, a process that admits a causal unravelling with systems of bounded dimension at every step can be efficiently represented by a tensor network state [36, 37], for which tomography can be performed efficiently [38]. In a quantum communication network, efficient tomography of the transmission paths is crucial for the design of encoding, decoding and calibration schemes for more efficient data transmission. In physics experiments, the causal structure and tomography data are useful for modelling the underlying physical process, for example, by finding the smallest quantum model that reproduces the observed data [39–41]. More generally, characterizing the causal structure of a multipartite process as a tensor network enables the use of efficient protocols that exploits the tensor network structure, including simulation protocols [37, 42, 43] and compression protocols [44].

IV. Methods

Efficient tests for the last tooth via the SWAP test. In the Results, we have given the framework of [Algorithm 1](#). In this section, we discuss how the tests for the last tooth, namely [line 5](#) of [Algorithm 1](#), can be carried out efficiently.

Consider a process \mathcal{C} of three input wires A_1, A_2, A_3 and three output wires B_1, B_2, B_3 , and suppose that we want to test whether (A_1, B_1) is the last tooth, which is equivalent to the independence test between A_1 and $A_2A_3B_2B_3$ according to [Proposition 1](#). Testing the independence between A_1 and $A_2A_3B_2B_3$ can be converted to the estimation of $\chi_1(A_1; A_2A_3B_2B_3)_C = \|C_{A_1A_2A_3B_2B_3} - C_{A_1} \otimes C_{A_2A_3B_2B_3}\|_1$, which is the distance between marginal Choi states. Each copy of $C_{A_1A_2A_3B_2B_3}$ or $C_{A_2A_3B_2B_3}$ can be prepared with one use of the process \mathcal{C} . Note that C_{A_1} equals to I_{A_1}/d_{A_1} by definition of a CPTP map. Given the ability to prepare the marginal Choi states, we now consider the estimation of their distance, which gives the value of $\chi_1(A_1; A_2A_3B_2B_3)_C$. In the following, we first talk about the estimation of another distance measure, the Hilbert-Schmidt distance, and use it to bound the trace distance as used by χ_1 .

Generally, the Hilbert-Schmidt distance between two states ρ and σ is defined as $\|\rho - \sigma\|_2$, where $\|X\|_2 := \sqrt{\text{Tr}[X^\dagger X]}$ denotes the Schatten 2-norm, also known as the Frobenius norm. It is related to the trace distance by the following inequality [45]:

$$2\|\rho - \sigma\|_2^2 \leq \|\rho - \sigma\|_1^2 \leq \frac{4\text{rank}(\rho)\text{rank}(\sigma)}{\text{rank}(\rho) + \text{rank}(\sigma)} \|\rho - \sigma\|_2^2. \quad (5)$$

The Hilbert-Schmidt distance between two quantum states can be estimated via SWAP tests [25]. The SWAP test uses the quantum circuit in [Figure 4](#) to estimate $\text{Tr}[\rho\sigma]$ for two given quantum states ρ and σ .

If we run the circuit in [Figure 4](#) for N times and let c_+ be the number of times observing outcome $|+\rangle$, then $2c_+/N - 1$ is an estimate of $\text{Tr}[\rho\sigma]$. The algorithm that yields an estimate of $\text{Tr}[\rho\sigma]$ is as follows, which produces an

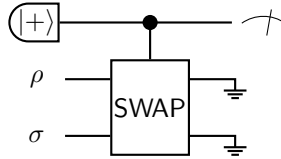


FIG. 4. **The SWAP test circuit.** The circuit consists of a controlled-SWAP gate with control qubit initialized to $|+\rangle$. Measuring the control system under the $\{|+\rangle, |-\rangle\}$ basis yields the outcome $|+\rangle$ with probability $(1 + \text{Tr}[\rho\sigma])/2$. The ground symbol means discarding the system.

estimate with error no more than ε with probability $1 - \kappa$ as shown in [Lemma 1](#).

Function 1: SWAPTEST($\rho, \sigma, \varepsilon, \kappa$)

Input : Quantum states ρ and σ (accessed by oracles that generate the states), error threshold ε , confidence κ

Output : Approximate value of $\text{Tr}[\rho\sigma]$

- 1 $N \leftarrow \lceil 2\varepsilon^{-2} \log(2/\kappa) \rceil$;
 - 2 Run the circuit in [Figure 4](#) for N times. Let c_+ be the number of outcome $|+\rangle$;
 - 3 Return $2c_+/N - 1$;
-

Lemma 1. *With probability $1 - \kappa$, the SWAP test estimates $\text{Tr}[\rho\sigma]$ within error ε .*

Proof. For each run, the probability that the outcome is $|+\rangle$ is $(1 + \text{Tr}[\rho\sigma])/2$. By Hoeffding's inequality,

$$\Pr \left[\left| \frac{c_+}{N} - \frac{1 + \text{Tr}[\rho\sigma]}{2} \right| \leq \varepsilon/2 \right] \geq 1 - 2e^{-\varepsilon^2 N/2}$$

$$\Pr [|2c_+/N - 1 - \text{Tr}[\rho\sigma]| \leq \varepsilon] \geq 1 - 2e^{-\varepsilon^2 (2\varepsilon^{-2} \log(2/\kappa))/2} = 1 - \kappa \quad (6)$$

□

The SWAP test is efficient in the sense that its circuit complexity is linear in the number of qubits representing the systems. For d -dimensional states ρ and σ , the controlled-SWAP gate acting on ρ and σ can be realized with $\lceil \log d \rceil$ controlled-SWAP gates acting on each pair of corresponding qubits of ρ and σ , and thus can be implemented with $O(\log d)$ gates.

Running SWAP tests on $\rho \otimes \sigma$, $\rho \otimes \rho$, and $\sigma \otimes \sigma$, we are able to obtain estimates for $\text{Tr}[\rho\sigma]$, $\text{Tr}[\rho^2]$ and $\text{Tr}[\sigma^2]$, respectively. From these estimates we can compute the Hilbert-Schmidt distance between ρ and σ according to the following equation:

$$\|\rho - \sigma\|_2^2 = \text{Tr}[\rho^2] + \text{Tr}[\sigma^2] - 2\text{Tr}[\rho\sigma]. \quad (7)$$

Coming back to the independence tests, by applying SWAP tests on marginal Choi states $C_{A_1 A_2 A_3 B_2 B_3}$ and $C_{A_1} \otimes C_{A_2 A_3 B_2 B_3}$, we can estimate their Hilbert-Schmidt distance. Using Eq. (5), we can bound their trace distance,

obtain a bound on $\chi_1(A_1; A_2A_3B_2B_3)_C$, determine the independence between A_1 and $A_2A_3B_2B_3$, and decide whether (A_1, B_1) is the last tooth. This procedure is summarized in [Function 2](#).

Function 2: `checklast`($\mathcal{C}, A_x, B_y, \varepsilon, \delta, \kappa$)

Input : A quantum channel \mathcal{C} , input wire A_x , output wire B_y , error thresholds ε, δ , confidence κ

Output : Whether (A_x, B_y) is the last tooth of \mathcal{C}

```

1  Prepare the circuits that generate the states  $C_1 := \text{Tr}_{B_y}[C]$  and  $C_2 := I_{A_x}/d_{A_x} \otimes \text{Tr}_{A_x B_y}[C]$ ;
2   $p_1 \leftarrow \text{SWAPTEST}(C_1, C_1, \varepsilon, \kappa)$  ;
3   $p_2 \leftarrow \text{SWAPTEST}(C_2, C_2, \varepsilon, \kappa)$  ;
4   $p_3 \leftarrow \text{SWAPTEST}(C_1, C_2, \varepsilon, \kappa)$  ;
5  if  $p_1 + p_2 - 2p_3 > \delta$  then                                // The estimated distance is larger than  $\delta$ 
6  |   Return false;                                           //  $(A_x, B_y)$  is not the last tooth
7  else
8  |   Return true;                                           //  $(A_x, B_y)$  is the last tooth
9  end

```

This completes [Algorithm 1](#). The choices of ε and δ are done in the detailed error analysis in [Supplementary Note 2](#). To ensure the correctness and efficiency, we need to further ensure that Eq. (5) provides a useful bound by giving upper bounds on the ranks of the marginal Choi states. Such upper bounds can be obtained from [Assumption 1](#), and the details are in [Supplementary Note 2](#).

We have shown the possibility of using the SWAP test as an efficient test of independence. The SWAP test could in principle be replaced by any algorithm for estimating the Hilbert-Schmidt distance, with possibly lower sample complexity [46]. In a quantum network scenario, causal unravelling may be performed by multiple parties, each of which has access to one input system or one output system. A bonus of the SWAP test is that, since a controlled-SWAP gate for two multipartite states can be decomposed into controlled-SWAP gates on the local systems of each party, only the control qubit needs to be transferred from one party to another in each round of the test. Additionally, the control qubit is measured after each round, and therefore parties do not need to carry quantum memories over subsequent rounds.

Testing the independence between all input-output pairs. In this section, we show the algorithm to test the independence between every pair of input and output wires, resulting in a Boolean matrix ind_{ij} . The first step is to collect statistics of the channel \mathcal{C} . When collecting data, we need to ensure that the information encoded in the quantum data are preserved, for which purpose we use informationally complete POVMs [47]. The elements of such a POVM on Hilbert space \mathcal{H} form a spanning set of $L(\mathcal{H})$, and the number of elements can be chosen as $(\dim \mathcal{H})^2$.

We pick an informationally complete POVM $\{P_{A_i, \alpha}\}_{\alpha=1}^{d_{A_i}^2}$ for each input wire A_i and $\{Q_{B_j, \beta}\}_{\beta=1}^{d_{B_j}^2}$ for each output wire B_j . We pick N to be the number of queries to the channel \mathcal{C} . In each query, we measure the Choi state of \mathcal{C}

with the POVM

$$\{P_{A_1, \alpha_1} \otimes \cdots \otimes P_{A_n, \alpha_n} \otimes Q_{B_1, \beta_1} \otimes \cdots \otimes Q_{B_n, \beta_n}\}_{\alpha_1, \dots, \alpha_n, \beta_1, \dots, \beta_n} \quad (8)$$

This POVM can be realized with local measurements on each wire. Let $(\alpha_1^{(k)}, \dots, \alpha_n^{(k)}, \beta_1^{(k)}, \dots, \beta_n^{(k)})$ be the outcome of the k -th query. We can write the outcomes in a matrix as shown in Figure 5.

k	A_1	\cdots	A_i	\cdots	A_n	B_1	\cdots	B_j	\cdots	B_n
1	$\alpha_1^{(1)}$	\cdots	$\alpha_i^{(1)}$	\cdots	$\alpha_n^{(1)}$	$\beta_1^{(1)}$	\cdots	$\beta_j^{(1)}$	\cdots	$\beta_n^{(1)}$
2	$\alpha_1^{(2)}$	\cdots	$\alpha_i^{(2)}$	\cdots	$\alpha_n^{(2)}$	$\beta_1^{(2)}$	\cdots	$\beta_j^{(2)}$	\cdots	$\beta_n^{(2)}$
\vdots	\vdots	\ddots	\vdots	\ddots	\vdots	\vdots	\ddots	\vdots	\ddots	\vdots
N	$\alpha_1^{(N)}$	\cdots	$\alpha_i^{(N)}$	\cdots	$\alpha_n^{(N)}$	$\beta_1^{(N)}$	\cdots	$\beta_j^{(N)}$	\cdots	$\beta_n^{(N)}$

FIG. 5. **Matrix of measurement outcomes.** Each row corresponds to a query to the process, and each column corresponds to an input or output wire. When we investigate A_i and B_j , we only look at the corresponding columns in the matrix and check the independence from data in these columns.

This matrix will be used to determine the independence between every pair of input and output wires. When we investigate A_i and B_j , we only look at the corresponding columns in the matrix and check the independence from data in these columns. Since we are using an informationally complete POVM, the independence between the two columns of the matrix is equivalent to the independence between the input A_i and output B_j . With this idea, we will be able to compute a Boolean matrix ind_{ij} such that $\text{ind}_{ij} = \text{true}$ if and only if A_i and B_j are independent, up to an error related to N , the number of queries.

One may notice that the POVM in Eq. (8) is enough for a full process tomography of \mathcal{C} . This is true if we pick an exponentially large N as large as the square of the product of all input and output dimensions. However, to compute ind_{ij} with a small error, N does not need to be large. We show that N could be chosen to grow only logarithmically with n , far less than a full process tomography.

Lemma 2. *Given a channel \mathcal{C} with input wires A_1, \dots, A_n and output wires B_1, \dots, B_n , there exists an algorithm that satisfies the following conditions:*

1. *With probability $1 - n^2\kappa_0$, the algorithm produces an output satisfying:*

(a) *if $\text{ind}_{i,j} = \text{false}$, then $\chi_1(C_{A_i, B_j}) > \chi_- - \varepsilon_0$*

(b) *if $\text{ind}_{i,j} = \text{true}$, then $\chi_1(C_{A_i, B_j}) \leq \chi_- + \varepsilon_0$*

where $\chi_- > 0$ is a threshold that can be freely chosen.

2. The number of queries to C is in the order of

$$N = O(d_A^6 d_B^6 \varepsilon_0^{-2} \log(d_A d_B \kappa_0^{-1})) . \quad (9)$$

The detailed algorithm and the proof are in [Supplementary Note 3](#).

The Boolean matrix ind_{ij} gives a partial order of the wires: if $\text{ind}_{ij} = \mathbf{false}$, then A_i must be before B_j . This partial order may not produce the full ordering of the wires, but will be a convenient initial guess for the causal unravelling, since its complexity is much lower than the general algorithm [Algorithm 1](#) for large n . In the Results, we show that under Assumptions [3](#) or [4](#), this partial order is enough to infer the full order.

Furthermore, the matrix of outcomes ([Figure 5](#)) is a conversion from the quantum process to classical data, making it possible to adopt classical causal discovery algorithms [[1](#), [3–5](#)]. For example, one could use algorithms based on the graph model, and try to find a graph in the form of [Figure 3](#) that best fits the observation data in [Figure 5](#).

V. Data availability

The authors declare that the data supporting the findings of this study are available within the paper and in the Supplementary Information files.

VI. Acknowledgements

This work was supported by the National Natural Science Foundation of China through grant 11675136, the Hong Kong Research Grant Council through grants 17300918 and 17307520, and through the Senior Research Fellowship Scheme SRFS2021-7S02, the Croucher Foundation, and the John Templeton Foundation through grant 61466, The Quantum Information Structure of Spacetime (qiss.fr). Research at the Perimeter Institute is supported by the Government of Canada through the Department of Innovation, Science and Economic Development Canada and by the Province of Ontario through the Ministry of Research, Innovation and Science. The opinions expressed in this publication are those of the authors and do not necessarily reflect the views of the John Templeton Foundation. The work of M. Hayashi was supported in part by Guangdong Provincial Key Laboratory (Grant No. 2019B121203002).

VII. Author contributions

G.B., Y.-D.W., Y.Z. and G.C. contributed to the development of the first algorithm. M.H. and G.B. proposed and refined the algorithms with local observations. G.C. proposed the problem and supervised this project. All authors discussed extensively the research presented in this paper and contributed to the writing of this manuscript.

VIII. Competing interests

The Authors declare no Competing Financial or Non-Financial Interests.

-
- [1] Peter Spirtes, Clark N Glymour, Richard Scheines, and David Heckerman. *Causation, prediction, and search*. MIT press, 2000.
- [2] Judea Pearl. *Causality*. Cambridge university press, 2009.
- [3] Christina Heinze-Deml, Marloes H Maathuis, and Nicolai Meinshausen. Causal structure learning. *Annual Review of Statistics and Its Application*, 5:371–391, 2018.
- [4] David Maxwell Chickering. Optimal structure identification with greedy search. *Journal of machine learning research*, 3:507–554, 2002.
- [5] Ioannis Tsamardinos, Laura E Brown, and Constantin F Aliferis. The max-min hill-climbing bayesian network structure learning algorithm. *Machine learning*, 65:31–78, 2006.
- [6] David Maxwell Chickering. Learning bayesian networks is np-complete. In *Learning from data*, pages 121–130. Springer, 1996.
- [7] Max Chickering, David Heckerman, and Chris Meek. Large-sample learning of bayesian networks is np-hard. *Journal of Machine Learning Research*, 5:1287–1330, 2004.
- [8] Christopher J Wood and Robert W Spekkens. The lesson of causal discovery algorithms for quantum correlations: Causal explanations of bell-inequality violations require fine-tuning. *New Journal of Physics*, 17(3):033002, 2015.
- [9] Thomas Van Himbeek, Jonatan Bohr Brask, Stefano Pironio, Ravishankar Ramanathan, Ana Belén Sainz, and Elie Wolfe. Quantum violations in the instrumental scenario and their relations to the bell scenario. *Quantum*, 3:186, 2019.
- [10] Joe Henson, Raymond Lal, and Matthew F Pusey. Theory-independent limits on correlations from generalized bayesian networks. *New Journal of Physics*, 16(11):113043, 2014.
- [11] Jacques Pienaar and Časlav Brukner. A graph-separation theorem for quantum causal models. *New Journal of Physics*, 17(7):073020, 2015.
- [12] Fabio Costa and Sally Shrapnel. Quantum causal modelling. *New Journal of Physics*, 18(6):063032, 2016.
- [13] John-Mark A Allen, Jonathan Barrett, Dominic C Horsman, Ciarán M Lee, and Robert W Spekkens. Quantum common causes and quantum causal models. *Physical Review X*, 7(3):031021, 2017.
- [14] Jonathan Barrett, Robin Lorenz, and Ognjan Oreshkov. Quantum causal models. *arXiv preprint arXiv:1906.10726*, 2019.
- [15] Jonathan Barrett, Robin Lorenz, and Ognjan Oreshkov. Cyclic quantum causal models. *Nat. Commun.*, 12:885, 2021.
- [16] Katja Ried, Megan Agnew, Lydia Vermeyden, Dominik Janzing, Robert W Spekkens, and Kevin J Resch. A quantum advantage for inferring causal structure. *Nature Physics*, 11:414–420, 2015.
- [17] Joseph F Fitzsimons, Jonathan A Jones, and Vlatko Vedral. Quantum correlations which imply causation. *Scientific reports*, 5:1–7, 2015.
- [18] Giulio Chiribella and Daniel Ebler. Quantum speedup in the identification of cause–effect relations. *Nature communications*, 10:1472, 2019.
- [19] Christina Giarmatzi and Fabio Costa. A quantum causal discovery algorithm. *NPJ Quantum Information*, 4:1–9, 2018.

- [20] Felix A Pollock, César Rodríguez-Rosario, Thomas Frauenheim, Mauro Paternostro, and Kavan Modi. Operational markov condition for quantum processes. *Physical review letters*, 120(4):040405, 2018.
- [21] Graeme D Berk, Andrew JP Garner, Benjamin Yadin, Kavan Modi, and Felix A Pollock. Resource theories of multi-time processes: A window into quantum non-markovianity. *Quantum*, 5:435, 2021.
- [22] Giulio Chiribella, G Mauro D’Ariano, and Paolo Perinotti. Quantum circuit architecture. *Physical Review Letters*, 101(6):060401, 2008.
- [23] Giulio Chiribella, Giacomo Mauro D’Ariano, and Paolo Perinotti. Theoretical framework for quantum networks. *Physical Review A*, 80(2):022339, 2009.
- [24] Gus Gutoski, Patrick Hayden, Kevin Milner, and Mark M Wilde. Quantum interactive proofs and the complexity of separability testing. *Theory of Computing*, 11(3):59, 2015.
- [25] Harry Buhrman, Richard Cleve, John Watrous, and Ronald De Wolf. Quantum fingerprinting. *Physical Review Letters*, 87(16):167902, 2001.
- [26] Man-Duen Choi. Completely positive linear maps on complex matrices. *Linear algebra and its applications*, 10(3):285–290, 1975.
- [27] Ding Jia. Quantifying causality in quantum and general models. *arXiv preprint arXiv:1801.06293*, 2018.
- [28] Alexei Yu Kitaev, Alexander Shen, Mikhail N Vyalyi, and Mikhail N Vyalyi. *Classical and quantum computation*. Number 47. American Mathematical Soc., 2002.
- [29] Pater Spirtes, Clark Glymour, Richard Scheines, Stuart Kauffman, Valerio Aimale, and Frank Wimberly. Constructing bayesian network models of gene expression networks from microarray data. 2000.
- [30] H Jeff Kimble. The quantum internet. *Nature*, 453(7198):1023–1030, 2008.
- [31] Chip Elliott. Building the quantum network. *New Journal of Physics*, 4(1):46, 2002.
- [32] Stephanie Wehner, David Elkouss, and Ronald Hanson. Quantum internet: A vision for the road ahead. *Science*, 362(6412), 2018.
- [33] David B Johnson and David A Maltz. Dynamic source routing in ad hoc wireless networks. In *Mobile computing*, pages 153–181. Springer, 1996.
- [34] Elizabeth M Royer and Chai-Keong Toh. A review of current routing protocols for ad hoc mobile wireless networks. *IEEE personal communications*, 6(2):46–55, 1999.
- [35] Ge Bai and Giulio Chiribella. Test one to test many: a unified approach to quantum benchmarks. *Physical Review Letters*, 120(15):150502, 2018.
- [36] Mark Fannes, Bruno Nachtergaele, and Reinhard F Werner. Finitely correlated states on quantum spin chains. *Communications in Mathematical Physics*, 144(3):443–490, 1992.
- [37] Frank Verstraete, Valentin Murg, and J Ignacio Cirac. Matrix product states, projected entangled pair states, and variational renormalization group methods for quantum spin systems. *Advances in Physics*, 57(2):143–224, 2008.
- [38] Marcus Cramer, Martin B Plenio, Steven T Flammia, Rolando Somma, David Gross, Stephen D Bartlett, Olivier Landon-Cardinal, David Poulin, and Yi-Kai Liu. Efficient quantum state tomography. *Nature communications*, 1:149, 2010.
- [39] Mile Gu, Karoline Wiesner, Elisabeth Rieper, and Vlatko Vedral. Quantum mechanics can reduce the complexity of classical models. *Nature communications*, 3:762, 2012.

- [40] Alex Monras and Andreas Winter. Quantum learning of classical stochastic processes: The completely positive realization problem. *Journal of Mathematical Physics*, 57(1):015219, 2016.
- [41] Jayne Thompson, Andrew JP Garner, Vlatko Vedral, and Mile Gu. Using quantum theory to simplify input–output processes. *npj Quantum Information*, 3(6):1–8, 2017.
- [42] Y-Y Shi, L-M Duan, and Guifre Vidal. Classical simulation of quantum many-body systems with a tree tensor network. *Physical review a*, 74(2):022320, 2006.
- [43] Guifré Vidal. Class of quantum many-body states that can be efficiently simulated. *Physical Review Letters*, 101(11):110501, 2008.
- [44] Ge Bai, Yuxiang Yang, and Giulio Chiribella. Quantum compression of tensor network states. *New Journal of Physics*, 22(4):043015, 2020.
- [45] Patrick J Coles, M Cerezo, and Lukasz Cincio. Strong bound between trace distance and hilbert-schmidt distance for low-rank states. *Physical Review A*, 100(2):022103, 2019.
- [46] Costin Bădescu, Ryan O’Donnell, and John Wright. Quantum state certification. In *Proceedings of the 51st Annual ACM SIGACT Symposium on Theory of Computing*, pages 503–514, 2019.
- [47] E Prugovečki. Information-theoretical aspects of quantum measurement. *International Journal of Theoretical Physics*, 16(5):321–331, 1977.
- [48] Joseph M Renes, Robin Blume-Kohout, Andrew J Scott, and Carlton M Caves. Symmetric informationally complete quantum measurements. *Journal of Mathematical Physics*, 45(6):2171–2180, 2004.
- [49] Martin Plesch and Āaslav Brukner. Quantum-state preparation with universal gate decompositions. *Physical Review A*, 83(3):032302, 2011.
- [50] Asher Peres. *Quantum theory: concepts and methods*, volume 57. Springer Science & Business Media, 2006.
- [51] Mikko Möttönen, Juha J Vartiainen, Ville Bergholm, and Martti M Salomaa. Quantum circuits for general multiqubit gates. *Physical review letters*, 93(13):130502, 2004.
- [52] Ryan O’Donnell and John Wright. Quantum spectrum testing. In *Proceedings of the forty-seventh annual ACM symposium on Theory of computing*, pages 529–538, 2015.

SUPPLEMENTARY NOTES

Supplementary Note 1 Preliminaries

In this section, we give the theoretical background of our algorithms.

In the main text, we showed that independence tests can be used to find the last tooth of a comb. Here we justify this idea by the following proposition that gives a sufficient and necessary condition for (A_x, B_y) to be the last tooth. The condition is based on the Choi state [26] of a channel, defined as $C \in \mathcal{H}_{A_1} \otimes \cdots \otimes \mathcal{H}_{A_n} \otimes \mathcal{H}_{B_1} \otimes \cdots \otimes \mathcal{H}_{B_n}$, $C := (C \otimes \mathcal{I})(|\Phi_+\rangle\langle\Phi_+|/d_{A_1, \dots, A_n})$ where $|\Phi_+\rangle := \sum_{i=1}^{d_{A_1, \dots, A_n}} |i\rangle_{A_1 \dots A_n} |i\rangle_{A_1 \dots A_n}$ is a maximally entangled state, $d_{A_1, \dots, A_n} := \prod_{i=1}^n d_{A_i}$ and $\{|i\rangle_{A_1 \dots A_n}\}_{i=1}^{d_{A_1, \dots, A_n}}$ is a basis of $\mathcal{H}_{A_1} \otimes \cdots \otimes \mathcal{H}_{A_n}$.

Proposition 2. [22] *Let C be the Choi state of a channel \mathcal{C} . (A_x, B_y) is the last tooth of \mathcal{C} in some causal unravelling*

of \mathcal{C} if and only if

$$C_{A_1, \dots, A_n, B \neq y} = C_{A \neq x, B \neq y} \otimes \frac{I_{A_x}}{d_{A_x}} \quad (10)$$

where $C_{A_1, \dots, A_n, B \neq y} := \text{Tr}_{B_y}[C]$, $C_{A \neq x, B \neq y} := \text{Tr}_{A_x B_y}[C]$, and I_{A_x} is the identity operator on system A_x .

The condition Eq. (10) for the Choi state C is equivalent to that for the process \mathcal{C} , the sets of systems $\{A_x\}$ and $\{A_i | i \neq x\} \cup \{B_j | j \neq y\}$ are independent.

When we collect classical statistics from a quantum state or process, we need to ensure that the information encoded in the quantum data are preserved, for which purpose we introduce the informationally complete POVM [47].

Definition 1. A POVM $\{P_\alpha\}$ on Hilbert space \mathcal{H} is informationally complete if its elements form a spanning set of linear operators on \mathcal{H} , namely for any $X \in L(\mathcal{H})$, there exist complex numbers $\{p_\alpha\}$ such that $X = \sum_\alpha p_\alpha P_\alpha$.

We say a set of states $\{\psi_\alpha\}$ is informationally complete if there exists an informationally complete POVM $\{P_\alpha\}$ such that $\psi_\alpha = P_\alpha / \text{Tr}[P_\alpha]$, $\forall \alpha$.

For efficiency considerations, we prefer to choose an informationally complete POVM with the minimal number of elements. To form a spanning set of $L(\mathcal{H})$, the minimal informationally complete POVM contains $(\dim \mathcal{H})^2$ elements, which are linearly independent. A typical example of such POVMs is the symmetric informationally complete POVM (SIC-POVM) [48], which has been found for most relevant low-dimensional Hilbert spaces.

The frame operators defined below will be used to characterize the sensitivity of measurement outcomes about the state being measured.

Definition 2. The frame operator of an informationally complete POVM $\{P_\alpha\}$ on Hilbert space \mathcal{H} is defined as $F := \sum_\alpha |P_\alpha\rangle\rangle \langle\langle P_\alpha| \in L(\mathcal{H} \otimes \mathcal{H})$, where $|P_\alpha\rangle\rangle := (P_\alpha \otimes I)|I\rangle\rangle = \sum_{i,j} (P_\alpha)_{ij} |i\rangle |j\rangle \in \mathcal{H} \otimes \mathcal{H}$, where $|I\rangle\rangle := \sum_i |i\rangle |i\rangle$ is the unnormalized maximally entangled state.

For an informationally complete set of states $\{\psi_\alpha\}$, the frame operator is defined as $F' := \sum_\alpha |\psi_\alpha\rangle\rangle \langle\langle \psi_\alpha|$ with $|\psi_\alpha\rangle\rangle := (\psi_\alpha \otimes I)|I\rangle\rangle$.

A frame operator with a larger minimum eigenvalue indicates that the outcome probabilities are more sensitive to any change of the state being measured, and the POVM is more efficient for obtaining the full information of the state. We will see the consequences of the minimum eigenvalue of frame operators in the analysis of our algorithms.

Supplementary Note 2 Proof of Theorem 1

We prove Theorem 1 in this section. In Supplementary Note 2 a, we analyze the accuracy of the independence tests in the approximate case. In Supplementary Note 2 b we analyze how the error in each recursion step affects the final error of the algorithm. The main proof of Theorem 1 is in Supplementary Note 2 c.

We assume that the process \mathcal{C} is already in its standard form with all input and output wires having dimension d_A , and thus $r_{\mathcal{C}} = \text{rank}(\mathcal{C})$.

a. Accuracy of independence tests

We first consider the accuracy of the independence test implemented in **Function 2**, in an arbitrary iteration of **Algorithm 1**. Define $C_1 := \text{Tr}_{B_y}[C]$ and $C_2 := I_{A_x}/d_{A_x} \otimes \text{Tr}_{A_x B_y}[C]$ as in **Function 2**. By **Lemma 1**, for each of the estimate p_i , ($i = 1, 2, 3$), with probability $1 - \kappa$, p_i is ε -close to the true value. By the union bound, with probability at least $1 - 3\kappa$, all three estimates are ε -close to their corresponding true values, and therefore

$$\begin{aligned} & |p_1 + p_2 - 2p_3 - \|C_1 - C_2\|_2^2| \\ & \leq |p_1 - \text{Tr}[C_1^2]| + |p_2 - \text{Tr}[C_2^2]| + |2p_3 - 2\text{Tr}[C_1 C_2]| \\ & \leq 4\varepsilon. \end{aligned} \tag{11}$$

Next, using Eq. (5),

$$\sqrt{2}\|C_1 - C_2\|_2 \leq \|C_1 - C_2\|_1 \leq \sqrt{\frac{4\text{rank}(C_1)\text{rank}(C_2)}{\text{rank}(C_1) + \text{rank}(C_2)}}} \|C_1 - C_2\|_2 \leq \sqrt{4\text{rank}(C_1)} \|C_1 - C_2\|_2 \tag{12}$$

The rank of C_1 can be bounded as

$$\text{rank}(C_1) = \text{rank}(\text{Tr}_{B_y}[C]) \leq d_{B_y} \text{rank}(C) = d_A \text{rank}(C) \tag{13}$$

Therefore by Eq. (12),

$$\sqrt{2}\|C_1 - C_2\|_2 \leq \|C_1 - C_2\|_1 \leq \sqrt{4d_A \text{rank}(C)} \|C_1 - C_2\|_2 \tag{14}$$

Now we consider the output of **Function 2**. If **Function 2** returns **true**, then $p_1 + p_2 - 2p_3 \leq \delta$. From Eq. (11), $\|C_1 - C_2\|_2 \leq \sqrt{\delta + 4\varepsilon}$ and then from Eq. (14), $\|C_1 - C_2\|_1 \leq \sqrt{4d_A \text{rank}(C)} \|C_1 - C_2\|_2 \leq \sqrt{4d_A \text{rank}(C)(\delta + 4\varepsilon)}$. If **Function 2** returns **false**, then $p_1 + p_2 - 2p_3 > \delta$, and thus $\|C_1 - C_2\|_1 \geq \sqrt{2} \|C_1 - C_2\|_2 > \sqrt{2(\delta - 4\varepsilon)}$. Since $\chi_1(A_x; A_{\neq x} B_{\neq y})_{\mathcal{C}} = \|C_1 - C_2\|_1$, we have the following lemma:

Lemma 3. *Let \mathcal{C} be the input channel of **Function 2**. With probability $1 - 3\kappa$, **Function 2** satisfies the following:*

1. If **Function 2** returns **true**, then

$$\chi_1(A_x; A_{\neq x} B_{\neq y})_{\mathcal{C}} \leq \sqrt{4d_A \text{rank}(C)(\delta + 4\varepsilon)}, \tag{15}$$

where $\text{rank}(C)$ is the Kraus rank of \mathcal{C} ;

2. If *Function 2* returns **false**, then

$$\chi_1(A_x; A_{\neq x} B_{\neq y})_C > \sqrt{2(\delta - 4\varepsilon)}. \quad (16)$$

b. *Bounding the rank during recursion*

In the following, we first give some lemmas on the Kraus rank of channels, and then prove [Lemma 5](#), which can be used in the inductive proof of [Theorem 1](#) to upper bound the rank of \mathcal{C} in any recursion.

Lemma 4. *For a constant channel $\mathcal{C} : S(\mathcal{H}_A) \rightarrow S(\mathcal{H}_B)$ satisfying $\mathcal{C}(X) = \text{Tr}[X]\sigma_B$, one has $\text{rank}(\sigma_B) = \text{rank}(\mathcal{C})/\dim \mathcal{H}_A$, where $\text{rank}(\mathcal{C})$ is the Kraus rank of channel \mathcal{C} .*

Proof. Since $\mathcal{C}(X) = \text{Tr}[X]\sigma_B$, the Choi state of \mathcal{C} is $C = I_A/d_A \otimes \sigma_B$. Then $\text{rank}(C) = \text{rank}(I_A)\text{rank}(\sigma_B)$, and $\text{rank}(\sigma_B) = \text{rank}(C)/\text{rank}(I_A) = \text{rank}(\mathcal{C})/\dim \mathcal{H}_A$. \square

Corollary 1. *If $\mathcal{C} \in \text{Comb}[(A_1, B_1), (A_2, B_2)]$, then $\text{rank}(\mathcal{C}_{A_1 \rightarrow B_1}) \leq \text{rank}(\mathcal{C})d_{B_2}/d_{A_2}$, where $\mathcal{C}_{A_1 \rightarrow B_1}$ is the channel obtained from \mathcal{C} by inputting the maximally mixed state to A_2 and discarding the output of B_2 .*

Proof. Define $\mathcal{C}_{A_2 \rightarrow A_1 B_1}$ as $\mathcal{C}_{A_2 \rightarrow A_1 B_1}(\rho) := \text{Tr}_{B_2}[(\mathcal{C} \otimes \mathcal{I}_{A_1})(\rho \otimes |I\rangle\langle I|_{A_1 A_1}/d_{A_1})]$, namely the map with Choi state equal to $C_{A_1 B_1 A_2} := \text{Tr}_{B_2}[C]$, having A_2 as the input and A_1, B_1 as outputs. $\mathcal{C} \in \text{Comb}[(A_1, B_1), (A_2, B_2)]$ indicates that $C_{A_1 B_1 A_2} = C_{A_1 B_1} \otimes C_{A_2}$, and thus $\mathcal{C}_{A_2 \rightarrow A_1 B_1}$ is a constant channel: $\mathcal{C}_{A_2 \rightarrow A_1 B_1}(\rho) = \text{Tr}[\rho]C_{A_1 B_1}$. By [Lemma 4](#), $\text{rank}(C_{A_1 B_1}) = \text{rank}(\mathcal{C}_{A_2 \rightarrow A_1 B_1})/d_{A_2}$. Then

$$\text{rank}(\mathcal{C}_{A_1 \rightarrow B_1}) = \text{rank}(C_{A_1 B_1}) = \text{rank}(\mathcal{C}_{A_2 \rightarrow A_1 B_1})/d_{A_2} = \text{rank}(\text{Tr}_{B_2}[C])/d_{A_2} \leq \text{rank}(\mathcal{C})d_{B_2}/d_{A_2} \quad (17)$$

\square

Lemma 5. *Let $\mathcal{C}^{(n)}$ be the initial value of \mathcal{C} in [Algorithm 1](#), and let $\mathcal{C}^{(k)}$, which has k input wires and k output wires, be the value of \mathcal{C} in the $(n - k + 1)$ -th recursive call of [Algorithm 1](#). Define the follow propositions:*

- $P(k)$: *in the $(n - k + 1)$ -th recursive call of [Algorithm 1](#), the pair (A_x, B_y) passing the test is indeed the last tooth, namely $\mathcal{C}^{(k)} \in \text{Comb}[(A_{\neq x}, B_{\neq y}), (A_x, B_y)]$, where $A_{\neq x}$ ($B_{\neq y}$) denotes all input (output) wires of $\mathcal{C}^{(k)}$ excluding A_x (B_y).*
- $Q(k)$: $\text{rank}(\mathcal{C}^{(k)}) \leq \text{rank}(\mathcal{C}^{(n)})$.

Then, under [Assumption 1](#), $Q(k) \wedge P(k) \Rightarrow Q(k - 1)$, for every $k = n, n - 1, \dots, 2$.

Proof. According to $P(k)$, $\mathcal{C}^{(k)} \in \text{Comb}[(A_{\neq x}, B_{\neq y}), (A_x, B_y)]$, and the following channel $\mathcal{C}_{A_x \rightarrow A_{\neq x} B_{\neq y}}^{(k)} : \mathcal{H}_{A_x} \rightarrow$

$\mathcal{H}_{B \neq y} \otimes \mathcal{H}_{A'_{\neq x}}$ is a constant channel:

$$\mathcal{C}_{A_x \rightarrow A_{\neq x} B_{\neq y}}^{(k)}(\rho_{A_x}) := \text{Tr}_{B_y} \left[\left(\mathcal{C}^{(k)} \otimes \mathcal{I}_{A'_{\neq x}} \right) \left(\bigotimes_{z \neq x} \frac{|I\rangle\rangle \langle\langle I|_{A_z A'_z}}{d_{A_z}} \otimes \rho_{A_x} \right) \right]$$

Since $\mathcal{C}_{A_x \rightarrow A_{\neq x} B_{\neq y}}^{(k)}$ is a constant channel, $\mathcal{C}_{A_x \rightarrow A_{\neq x} B_{\neq y}}^{(k)}(X) = \text{Tr}[X]C^{(k-1)}$, where $C^{(k-1)}$ equals to the Choi state of the updated channel $\mathcal{C}^{(k-1)}$. According to [Lemma 4](#), $\text{rank}(C^{(k-1)}) \leq \text{rank}(C^{(k)}) \dim \mathcal{H}_{B_y} / \dim \mathcal{H}_{A_x} = \text{rank}(C^{(k)})$, where we used $\dim \mathcal{H}_{A_x} = \dim \mathcal{H}_{B_y} = d_A$ since we have assumed that the process is in its standard form in [Assumption 1](#). By $Q(k)$, $\text{rank}(C^{(k)}) \leq \text{rank}(C^{(n)})$, thus $\text{rank}(C^{(k-1)}) \leq \text{rank}(C^{(k)}) \leq \text{rank}(C^{(n)})$ and $Q(k-1)$ holds. \square

c. Proof of [Theorem 1](#)

Now we are ready to prove [Theorem 1](#).

Proof of [Theorem 1](#). In [Algorithm 1](#), using the relation $T_{\text{test}}(n) \leq n^2 + T_{\text{test}}(n-1)$, we can find that there are $T_{\text{test}}(n) \leq n^3$ independence tests, each of which invokes three SWAP tests. Each SWAP test produces an estimate within error ε with probability no less than $1 - \kappa$ according to [Lemma 1](#). Let $\kappa = \kappa_0/3n^3$, and from now we assume all SWAP tests are within error ε , which has probability no less than $1 - 3n^3\kappa = 1 - \kappa_0$.

Let $\mathcal{C}^{(n)}$ be the initial value of \mathcal{C} in [Algorithm 1](#), and let $\mathcal{C}^{(k)}$, which has k input wires and k output wires, be the value of \mathcal{C} in the $(n-k+1)$ -th recursive call of [Algorithm 1](#).

Consider testing whether (A_x, B_y) is the last tooth of $\mathcal{C}^{(k)}$ with [Function 2](#). Let S be the set of all wires of $\mathcal{C}^{(k)}$ excluding A_x and B_y . If (A_x, B_y) passes the test, namely [Function 2](#) returns **true**, by [Lemma 3](#),

$$\chi_1(A_x; S)_{\mathcal{C}^{(k)}} \leq \sqrt{4d_A \text{rank}(\mathcal{C}^{(k)})}(\delta + 4\varepsilon). \quad (18)$$

Now we pick $\delta \leq \frac{\chi_{\min}^2}{8d_A \text{rank}(\mathcal{C}^{(k)})}$ and $\varepsilon = \delta/5$. Eq. (18) then indicates $\chi_1(A_x; S)_{\mathcal{C}^{(k)}} \leq \sqrt{4d_A \text{rank}(\mathcal{C}^{(k)})}(\delta + 4\varepsilon) < \chi_{\min}$.

Since $\chi_1(A_x; S)_{\mathcal{C}^{(k)}} = \chi_1(A_x; S)_{\mathcal{C}^{(n)}}$, by [Assumption 2](#), $\chi_1(A_x; S)_{\mathcal{C}^{(k)}} = 0$. Therefore, if [Function 2](#) returns **true**, then (A_x, B_y) must be the last tooth of the comb, in some causal unravelling of $\mathcal{C}^{(k)}$. Using the notation in [Lemma 5](#), $P(k)$ holds for this iteration. On the other hand, if [Function 2](#) returns **false**, by [Lemma 3](#),

$$\chi_1(A_x; S)_{\mathcal{C}^{(n)}} = \chi_1(A_x; S)_{\mathcal{C}^{(k)}} > \sqrt{2(\delta - 4\varepsilon)} > 0, \quad (19)$$

and (A_x, B_y) does not satisfy the condition for being last tooth of the comb.

Let $r_{\mathcal{C}} := \text{rank}(\mathcal{C}^{(n)})$. Take the definition of $P(k)$ and $Q(k)$ from [Lemma 5](#). Now we perform an induction to prove $P(k)$ and $Q(k)$ for every k .

First, $Q(n)$ obviously holds according to [Assumption 1](#). Now, we assume that $Q(k)$ holds, and want to show that $Q(k-1)$ also holds.

By $Q(k)$, we have $\text{rank}(\mathcal{C}^{(k)}) \leq r_C$. In any recursive call of [Algorithm 1](#), if $Q(k)$ holds, then we can choose $\delta = \frac{\chi_{\min}^2}{8d_A r_C} \leq \frac{\chi_{\min}^2}{8d_A \text{rank}(\mathcal{C}^{(k)})}$, and by the argument above, $P(k)$ holds. Combining this with [Lemma 5](#), we have $Q(k) \Rightarrow P(k)$ and $Q(k) \wedge P(k) \Rightarrow Q(k-1)$, meaning $Q(k) \Rightarrow Q(k-1)$.

This completes the induction, and we conclude that $Q(k)$ and $P(k)$ holds for every k . $P(k)$ being true for every k shows the correctness of our algorithm.

According to [Function 1](#), $N = O(\varepsilon^{-2} \log \kappa^{-1}) = O(\delta^{-2} \log(n\kappa_0^{-1})) = O(d_A^2 r_C^2 \chi_{\min}^{-4} \log(n\kappa_0^{-1}))$. The sample complexity is then

$$T_{\text{sample}} = NT_{\text{test}}(n) = O(n^3 d_A^2 r_C^2 \chi_{\min}^{-4} \log(n\kappa_0^{-1})) \quad (20)$$

and the computational complexity is $O(T_{\text{sample}} n \log d_A)$ from the realization of SWAP tests. □

Supplementary Note 3 Independence test algorithm between all input-output pairs

In this section, we show the details of the algorithm to test the independence between every pair of input and output wires, resulting in a Boolean matrix ind_{ij} . Our independence test algorithm will be based on the estimation of $\chi_1(\rho_{A,B})$. The idea is essentially quantum state tomography: measure ρ_{AB} with informationally complete POVMs $\{P_\alpha\}$ on system A and $\{Q_\beta\}$ on system B , use the outcome statistics to reconstruct ρ_{AB} , and estimate $\chi_1(\rho_{A,B})$ based on the reconstructed state. The algorithm is given in [Function 3](#).

Function 3: estimatechi1 ($\{(a^{(k)}, b^{(k)})\}_{k=1}^N, \{P_\alpha\}, \{Q_\beta\}$)

Input : N measurement outcomes $\{(a^{(k)}, b^{(k)})\}_{k=1}^N$ of POVM $\{P_\alpha \otimes Q_\beta\}$ on state ρ_{AB}

Output : An estimate of $\chi_1(\rho_{A,B})$

- 1 Initialize $\hat{p}_{\alpha\beta}$ to zero for all $\alpha = 1, \dots, d_A^2$, and $\beta = 1, \dots, d_B^2$;
 - 2 **for** $k \leftarrow 1$ **to** N **do**
 - 3 $\hat{p}_{a^{(k)}b^{(k)}} \leftarrow \hat{p}_{a^{(k)}b^{(k)}} + 1/N$;
 - 4 **end**
 - 5 $F \leftarrow \sum_\alpha |P_\alpha\rangle\rangle \langle\langle P_\alpha|$;
 - 6 $G \leftarrow \sum_\beta |Q_\beta\rangle\rangle \langle\langle Q_\beta|$;
 - 7 $S \leftarrow \sum_\alpha |\alpha\rangle\rangle \langle\langle P_\alpha|$, where $\{|\alpha\rangle\rangle\}$ is a set of orthonormal vectors indexed by α ;
 - 8 $R \leftarrow \sum_\beta |\beta\rangle\rangle \langle\langle Q_\beta|$, where $\{|\beta\rangle\rangle\}$ is a set of orthonormal vectors indexed by β ;
 - 9 $|\hat{p}\rangle\rangle \leftarrow \sum_{\alpha,\beta} \hat{p}_{\alpha\beta} |\alpha\rangle\rangle |\beta\rangle\rangle$;
 - 10 Compute operator $\hat{\rho}_{AB}$ by $|\hat{\rho}_{AB}\rangle\rangle = (F^{-1}S^\dagger \otimes G^{-1}R^\dagger) |\hat{p}\rangle\rangle$;
 - 11 Return $\chi_1(\hat{\rho}_{A,B})$;
-

Now we analyze the accuracy and complexity of [Function 3](#). Define the constant $\xi := \frac{\sqrt{\lambda_{\min}(F)\lambda_{\min}(G)}}{\sqrt{d_A^2 d_B^2 + 4d_B^2 + 4d_A^2} d_A d_B}$ where

$\lambda_{\min}(X)$ denotes the minimum eigenvalue of operator X and F and G are defined in [Function 3](#). Then we define

$$\kappa(\varepsilon) := 2(d_A^2 d_B^2 + d_A^2 + d_B^2)e^{-2\xi^2 \varepsilon^2 N}. \quad (21)$$

The error of the estimate $\chi_1(\hat{\rho}_{A,B})$ is given in the following lemma, whose proof is in [Supplementary Note 3 a](#).

Lemma 6. *For any positive real number $\varepsilon > 0$, over the N measurement outcomes on independent copies of $\rho_{A,B}$, with probability $1 - \kappa_0$, the output of [Function 3](#) estimates $\chi_1(\rho_{A,B})$ with the following error bound*

$$|\chi_1(\rho_{A,B}) - \chi_1(\hat{\rho}_{A,B})| \leq \varepsilon. \quad (22)$$

That is, the inequality

$$\Pr(|\chi_1(\rho_{A,B}) - \chi_1(\hat{\rho}_{A,B})| > \varepsilon) \leq \kappa(\varepsilon) \quad (23)$$

holds for any positive real number $\varepsilon > 0$. Here, $\Pr(C)$ expresses the probability that the condition C is satisfied.

In other words, to reach confidence $1 - \kappa_0$ and error ε_0 , the number of samples N is of order

$$N = O(d_A^4 d_B^4 \lambda_{\min}^{-1}(F) \lambda_{\min}^{-1}(G) \varepsilon_0^{-2} \log(d_A d_B \kappa_0^{-1})). \quad (24)$$

If one choose $\{P_\alpha\}$ and $\{Q_\beta\}$ to be SIC-POVMs, $\lambda_{\min}^{-1}(F) = d_A(d_A + 1) = O(d_A^2)$ and $\lambda_{\min}^{-1}(G) = d_B(d_B + 1) = O(d_B^2)$ [48]. In this case, the number of samples $N = O(d_A^6 d_B^6 \varepsilon_0^{-2} \log(d_A d_B \kappa_0^{-1}))$ is polynomial in d_A and d_B .

[Function 3](#) could be used on quantum channels to discover the correlation between input and output wires. To characterize a quantum channel, we could transform it to its Choi state by feeding the input with half of a maximally entangled state, and apply [Function 3](#) on the Choi state. To save the cost of creating and maintaining entangled states, we could use [Function 3](#) in an alternative way. Let $\{\psi_\alpha\}_{\alpha=1}^{d_A^2}$ be an informationally complete set of states such that $\psi_\alpha = P_\alpha^T / \text{Tr}[P_\alpha]$. One samples ψ_α from $\{\psi_\alpha\}_{\alpha=1}^{d_A^2}$ with probability $\text{Tr}[P_\alpha]/d_A$, apply quantum channel $\mathcal{C} : L(\mathcal{H}_A) \rightarrow L(\mathcal{H}_B)$ on ψ_α , and measure the output with $\{Q_\beta\}_{\beta=1}^{d_B^2}$. This process generates the same statistics for (α, β) according to the following equation:

$$\frac{1}{d_A} \text{Tr}[P_\alpha] \text{Tr}[Q_\beta \mathcal{C}(\psi_\alpha)] = \frac{1}{d_A} \text{Tr}[Q_\beta \mathcal{C}(P_\alpha^T)] = \text{Tr} \left[\frac{1}{d_A} \sum_{i,j} P_\alpha |i\rangle \langle j| \otimes Q_\beta \mathcal{C}(|i\rangle \langle j|) \right] = \text{Tr}[(P_\alpha \otimes Q_\beta) C] \quad (25)$$

where $C := \frac{1}{d_A} \sum_{i,j} |i\rangle \langle j| \otimes \mathcal{C}(|i\rangle \langle j|)$ is the Choi state of channel \mathcal{C} . The left hand side of Eq. (25) is the probability of sampling ψ_α times the probability of outcome β on the output conditioned on the input being ψ_α , and the right hand side of Eq. (25) is the probability of outcome (α, β) if one measure the Choi state C with POVM $\{P_\alpha \otimes Q_\beta\}$.

Now we adopt [Function 3](#) to causal unravelling. By testing the correlation between every pair of input and output

wires, one is able to infer the causal unravellings: if output B_j is correlated to input A_i , B_j must be after A_i . In this section, we study cases where such reasoning yields the full causal unravelling.

We introduce an algorithm that discovers the correlations between every pair of input and output wires. The idea is to first collect all the required classical data, and deduce all the correlations according to the statistics. During this procedure, the data are reused for different input-output pairs, leading to fewer queries to the channel \mathcal{C} .

Function 4: independence(\mathcal{C}, N, χ_-)

Input : Black-box access of a quantum comb \mathcal{C} with input wires A_1, \dots, A_n and output wires B_1, \dots, B_n

Output : An array `ind` where `indi,j` being **true** indicates A_i and B_j are independent

- 1 Pick informationally complete linearly independent POVMs $\{P_\alpha^i\}_{\alpha=1}^{d_{A_i}^2}$ for each input A_i and $\{Q_\beta^j\}_{\beta=1}^{d_{B_j}^2}$ for each output B_j ;
 - 2 Define $\psi_\alpha^i := (P_\alpha^i)^T / \text{Tr}[P_\alpha^i]$, $\forall i = 1, \dots, n$, $\alpha = 1, \dots, d_{A_i}^2$;
 - 3 Generate N random n -tuples $\{(a_1^{(k)}, a_2^{(k)}, \dots, a_n^{(k)})\}_{k=1}^N$ where $a_i^{(k)}$ is chosen from $\{1, \dots, d_{A_i}^2\}$ with probability $\Pr(a_i^{(k)} = \alpha) = \text{Tr}[P_\alpha^i] / d_{A_i}$;
 - 4 **for** $k \leftarrow 1$ **to** N **do**
 - 5 Apply \mathcal{C} to input state $\psi_{a_1^{(k)}}^1 \otimes \psi_{a_2^{(k)}}^2 \cdots \otimes \psi_{a_n^{(k)}}^n$;
 - 6 For each j , measure j -th output wire with $\{Q_\beta^j\}_{\beta=1}^{d_{B_j}^2}$. Let the outcomes be $(b_1^{(k)}, b_2^{(k)}, \dots, b_n^{(k)})$, $b_j^{(k)} \in \{1, \dots, d_{B_j}^2\}$;
 - 7 **end**
 - 8 **for** $i \leftarrow 1$ **to** n **do**
 - 9 **for** $j \leftarrow 1$ **to** n **do**
 - 10 **if** `estimatechi1`($\{(a_i^{(k)}, b_j^{(k)})\}_{k=1}^N, \{P_\alpha^i\}, \{Q_\beta^j\}\}) \leq \chi_-$ **then**
 - 11 `indi,j` \leftarrow **true** ;
 - 12 **else**
 - 13 `indi,j` \leftarrow **false** ;
 - 14 **end**
 - 15 **end**
 - 16 **end**
 - 17 Output `ind`;
-

To understand **Function 4**, we observe that $\{(a_i^{(k)}, b_j^{(k)})\}_{k=1}^N$ are sampled from the same distribution as the outcomes of measuring C_{A_i, B_j} with $\{P_\alpha^i \otimes Q_\beta^j\}$, and `estimatechi1` produces an estimate of $\chi_1(A_i; B_j)_C$. Conditioned on that all n^2 number of calls to `estimatechi1` succeed, which has probability no less than $1 - n^2 \kappa_0$, all the estimations $\chi_1(A_i; B_j)_C$ have error no greater than ε_0 . We summarize these observations in the following lemma:

Lemma 7. *With probability $1 - n^2 \kappa_0$, **Function 4** produces an output satisfying:*

1. *if `indi,j` is **false**, then $\chi_1(C_{A_i, B_j}) > \chi_- - \varepsilon_0$*

2. if $\text{ind}_{i,j} = \mathbf{true}$, then $\chi_1(C_{A_i, B_j}) \leq \chi_- + \varepsilon_0$

where κ_0 and ε_0 are related as

$$\kappa_0 = 2(d_A^2 d_B^2 + d_A^2 + d_B^2) e^{-2\xi^2 \varepsilon_0^2 N}. \quad (26)$$

where $\xi := \frac{\sqrt{\lambda_{\min, \text{in}} \lambda_{\min, \text{out}}}}{\sqrt{d_A^2 d_B^2 + 4d_B^2 + 4d_A^2 d_A d_B}}$, $\lambda_{\min, \text{in}} := \min \lambda_{\min}(F_i)$, $\lambda_{\min, \text{out}} := \min \lambda_{\min}(G_i)$, and F_i (G_i) is the frame operator of $\{P_\alpha^i\}_{\alpha=1}^{d_{A_i}^2}$ ($\{Q_\beta^j\}_{\beta=1}^{d_{B_j}^2}$).

Lemma 2 is a paraphrase of **Lemma 7** by rewriting Eq. (26) and choosing $\{P_\alpha^i\}_{\alpha=1}^{d_{A_i}^2}$ and $\{Q_\beta^j\}_{\beta=1}^{d_{B_j}^2}$ to be SIC-POVMs so that $\lambda_{\min, \text{in}} = O(d_A^2)$ and $\lambda_{\min, \text{out}} = O(d_B^2)$.

a. Proof of Lemma 6

Lemma 8. Let $\{P_\alpha\}$ be an informationally complete POVM and $F := \sum_\alpha |P_\alpha\rangle\langle P_\alpha|$ be its frame operator. For two Hermitian operators ρ and σ , define $p_\alpha := \text{Tr}[P_\alpha \rho]$ and $q_\alpha := \text{Tr}[P_\alpha \sigma]$. Then one has

$$\frac{\sum_\alpha (p_\alpha - q_\alpha)^2}{\lambda_{\max}(F)} \leq \|\rho - \sigma\|_2^2 \leq \frac{\sum_\alpha (p_\alpha - q_\alpha)^2}{\lambda_{\min}(F)}, \quad (27)$$

where $\|X\|_2 := \sqrt{\text{Tr}[X^\dagger X]}$ denotes the Schatten 2-norm, also known as the Frobenius norm, and $\lambda_{\max}(F)$ and $\lambda_{\min}(F)$ are the maximum and minimum eigenvalues of F , respectively.

Proof. Let $T := \rho - \sigma$ and $t_\alpha := p_\alpha - q_\alpha$. Then $t_\alpha = \text{Tr}[P_\alpha \rho] - \text{Tr}[P_\alpha \sigma] = \text{Tr}[P_\alpha T]$. Define the vector $|t\rangle := \sum_\alpha t_\alpha |\alpha\rangle$, and operator $S := \sum_\alpha |\alpha\rangle\langle P_\alpha|$, where $\{|\alpha\rangle\}$ is a set of orthonormal vectors indexed by α . Then one has $|t\rangle = S|T\rangle$ and $S^\dagger S = F$.

$$\sum_\alpha t_\alpha^2 = \langle t|t\rangle = \langle T|S^\dagger S|T\rangle = \langle T|F|T\rangle. \quad (28)$$

Since $\lambda_{\min}(F) \langle T|T\rangle \leq \langle T|F|T\rangle \leq \lambda_{\max}(F) \langle T|T\rangle$, we obtain

$$\lambda_{\min}(F) \langle T|T\rangle \leq \sum_\alpha t_\alpha^2 \leq \lambda_{\max}(F) \langle T|T\rangle, \quad (29)$$

which is equivalent to Eq. (27) since $\langle T|T\rangle = \|T\|_2^2$. \square

Proof of Lemma 6. Let $\hat{\rho}_A := \text{Tr}_B[\hat{\rho}_{AB}]$ and $\hat{\rho}_B := \text{Tr}_A[\hat{\rho}_{AB}]$ be the marginal states of the reconstructed state $\hat{\rho}_{AB}$. Define $\tau := \rho_{AB} - \rho_A \otimes \rho_B$ and $\hat{\tau} := \hat{\rho}_{AB} - \hat{\rho}_A \otimes \hat{\rho}_B$, the error of **Function 3** is then the difference between $\|\tau\|_1 = \chi_1(A; B)_\rho$ and $\|\hat{\tau}\|_1 = \chi_1(A; B)_{\hat{\rho}}$.

Let $p_{\alpha\beta} := \text{Tr}[(P_\alpha \otimes Q_\beta)\rho_{AB}]$, $p_\alpha^A := \sum_\beta p_{\alpha\beta}$ and $p_\beta^B = \sum_\alpha p_{\alpha\beta}$. Let $\hat{p}_\alpha^A := \sum_\beta \hat{p}_{\alpha\beta}$ and $\hat{p}_\beta^B = \sum_\alpha \hat{p}_{\alpha\beta}$. Over the N

measurement outcomes, $\hat{p}_{\alpha\beta}$ is the average of independent Bernoulli random variables, and has mean $p_{\alpha\beta}$. The same is true for \hat{p}_{α}^A and \hat{p}_{β}^B , whose means are p_{α}^A and p_{β}^B , respectively.

Let $\varepsilon_1 := \xi\varepsilon$. By Hoeffding's inequality,

$$\Pr(|p_{\alpha\beta} - \hat{p}_{\alpha\beta}| \leq \varepsilon_1) \geq 1 - 2e^{-2\varepsilon_1^2 N} \quad (30)$$

$$\Pr(|p_{\alpha}^A - \hat{p}_{\alpha}^A| \leq \varepsilon_1) \geq 1 - 2e^{-2\varepsilon_1^2 N} \quad (31)$$

$$\Pr(|p_{\beta}^B - \hat{p}_{\beta}^B| \leq \varepsilon_1) \geq 1 - 2e^{-2\varepsilon_1^2 N} \quad (32)$$

By the union bound,

$$\Pr[(\forall \alpha, \beta, |p_{\alpha\beta} - \hat{p}_{\alpha\beta}| \leq \varepsilon_1) \wedge (\forall \alpha, |p_{\alpha}^A - \hat{p}_{\alpha}^A| \leq \varepsilon_1) \wedge (\forall \beta, |p_{\beta}^B - \hat{p}_{\beta}^B| \leq \varepsilon_1)] \geq 1 - 2(d_A^2 d_B^2 + d_A^2 + d_B^2)e^{-2\varepsilon_1^2 N}, \quad (33)$$

namely with probability no less than $1 - 2(d_A^2 d_B^2 + d_A^2 + d_B^2)e^{-2\varepsilon_1^2 N} = 1 - \kappa(\varepsilon)$, all $(d_A^2 d_B^2 + d_A^2 + d_B^2)$ number of the following inequalities

$$|p_{\alpha\beta} - \hat{p}_{\alpha\beta}| \leq \varepsilon_1, \quad \forall \alpha, \beta \quad (34)$$

$$|p_{\alpha}^A - \hat{p}_{\alpha}^A| \leq \varepsilon_1, \quad \forall \alpha \quad (35)$$

$$|p_{\beta}^B - \hat{p}_{\beta}^B| \leq \varepsilon_1, \quad \forall \beta \quad (36)$$

are satisfied. We then analyze the estimation error of $\chi_1(A; B)_\rho$ in this case. Define $t_{\alpha\beta} := p_{\alpha\beta} - p_{\alpha}^A p_{\beta}^B$. By Eqs. (34-36),

$$|t_{\alpha\beta} - \hat{t}_{\alpha\beta}| = |p_{\alpha\beta} - \hat{p}_{\alpha\beta} - p_{\alpha}^A p_{\beta}^B + \hat{p}_{\alpha}^A \hat{p}_{\beta}^B| \quad (37)$$

$$\leq |p_{\alpha\beta} - \hat{p}_{\alpha\beta}| + |p_{\alpha}^A p_{\beta}^B - \hat{p}_{\alpha}^A \hat{p}_{\beta}^B| + |p_{\alpha}^A \hat{p}_{\beta}^B - \hat{p}_{\alpha}^A p_{\beta}^B| \quad (38)$$

$$\leq \varepsilon_1 + p_{\alpha}^A |p_{\beta}^B - \hat{p}_{\beta}^B| + |p_{\alpha}^A - \hat{p}_{\alpha}^A| \hat{p}_{\beta}^B \quad (39)$$

$$\leq (1 + p_{\alpha}^A + \hat{p}_{\beta}^B) \varepsilon_1 \quad (40)$$

Since $\sum_{\alpha} p_{\alpha}^A = \sum_{\beta} \hat{p}_{\beta}^B = 1$, we have

$$\sum_{\alpha, \beta} (t_{\alpha\beta} - \hat{t}_{\alpha\beta})^2 \leq \sum_{\alpha, \beta} (1 + p_{\alpha}^A + \hat{p}_{\beta}^B)^2 \varepsilon_1^2 \quad (41)$$

$$\leq \sum_{\alpha, \beta} (1 + 4p_{\alpha}^A + 4\hat{p}_{\beta}^B) \varepsilon_1^2 \quad (42)$$

$$= (d_A^2 d_B^2 + 4d_B^2 + 4d_A^2) \varepsilon_1^2 \quad (43)$$

Note that $t_{\alpha\beta} = \text{Tr}[(P_{\alpha} \otimes Q_{\beta})\tau]$ and $\hat{t}_{\alpha\beta} = \text{Tr}[(P_{\alpha} \otimes Q_{\beta})\hat{\tau}]$. Applying Lemma 8 to POVM $\{P_{\alpha} \otimes Q_{\beta}\}$ and operators

τ and $\hat{\tau}$, we obtain

$$\|\tau - \hat{\tau}\|_2^2 \leq \frac{\sum_{\alpha,\beta} (t_{\alpha\beta} - \hat{t}_{\alpha\beta})^2}{\lambda_{\min}(F \otimes G)} \leq \frac{(d_A^2 d_B^2 + 4d_B^2 + 4d_A^2)\varepsilon_1^2}{\lambda_{\min}(F)\lambda_{\min}(G)} \quad (44)$$

Using the inequality $\|X\|_1^2 \leq \text{rank}(X)\|X\|_2^2$ for any operator X [45], we have

$$\|\tau - \hat{\tau}\|_1 \leq \sqrt{\text{rank}(\tau - \hat{\tau})}\|\tau - \hat{\tau}\|_2 \leq d_A d_B \sqrt{\frac{d_A^2 d_B^2 + 4d_B^2 + 4d_A^2}{\lambda_{\min}(F)\lambda_{\min}(G)}} \varepsilon_1 = \varepsilon \quad (45)$$

which proves Eq. (22) since $|\|\tau\|_1 - \|\hat{\tau}\|_1| \leq \|\tau - \hat{\tau}\|_1$. \square

Supplementary Note 4 Details of the algorithm under Assumption 3

In this section, we give the pseudocode of the algorithm under Assumption 3 and discuss its correctness and efficiency.

Algorithm 2: Quantum causal unravelling algorithm under Assumption 3

Input : Black-box access of a quantum comb \mathcal{C} with input wires A_1, \dots, A_n and output wires B_1, \dots, B_n ,

number of queries N

Output : Ordering of inputs and outputs

```

1  ind  $\leftarrow$  independence( $\mathcal{C}, N, \chi_{\min}/2$ );
2  for  $k \leftarrow 1$  to  $n$  do
3  |    $c_A(k) \leftarrow |\{i | \text{ind}_{k,i} = \text{false}\}|$ ;
4  |    $c_B(k) \leftarrow |\{i | \text{ind}_{i,k} = \text{false}\}|$ ;
5  end
6  Sort  $\{A_1, \dots, A_n\}$  in descending order of  $c_A(k)$  as  $\{A_{\sigma(1)}, \dots, A_{\sigma(n)}\}$ ;
7  Sort  $\{B_1, \dots, B_n\}$  in ascending order of  $c_B(k)$  as  $\{B_{\pi(1)}, \dots, B_{\pi(n)}\}$ ;
8  Output  $(A_{\sigma(1)}, B_{\pi(1)}), \dots, (A_{\sigma(n)}, B_{\pi(n)})$ ;

```

Here the threshold χ_- is set to $\chi_- = \chi_{\min}/2$. Now we discuss the correctness and efficiency of Algorithm 2 by proving Theorem 2.

Proof of Theorem 2. Let $\varepsilon_0 = \chi_{\min}/3$ and $\kappa_0 = \kappa/n^2$. By Lemma 7, with probability $1 - n^2\kappa_0 = 1 - \kappa$, the independence tests produce the true answers: (i) if $\text{ind}_{i,j} = \text{true}$, then $\chi_1(A_i; B_j)_C \leq \chi_- + \varepsilon_0 < \chi_{\min}$, and according to Assumption 3, A_i and B_j are independent; (ii) if $\text{ind}_{i,j} = \text{false}$, then $\chi_1(A_i; B_j)_C > \chi_- - \varepsilon_0 > 0$, and according to Assumption 3, A_i and B_j are correlated. In this case, Assumption 3 further ensures that $c_A(1), \dots, c_A(n)$ ($c_B(1), \dots, c_B(n)$) are distinct and Algorithm 2 always gives the correct causal unravelling.

The running time of Algorithm 2 mostly attributes to Function 4. We first discuss how to choose N , the number of queries to \mathcal{C} . The relationship between N , ε_0 and κ_0 is given in Lemma 2 as $N = O(d_A^6 d_B^6 \varepsilon_0^{-2} \log(d_A d_B \kappa_0^{-1}))$. By

our choice of parameters $\varepsilon_0 = \chi_{\min}/3$ and $\kappa_0 = \kappa/n^2$, we have

$$N = O(d_A^6 d_B^6 \chi_{\min}^{-2} \log(nd_A d_B \kappa^{-1})). \quad (46)$$

To analyze the computational complexity, we consider the two main parts of **Function 4**: the query part and the estimation part. The query part invokes the channel N times, and each time n state preparation and n measurements are performed. Here we assume that state preparation on a d -dimensional Hilbert space takes time $O(d)$ [49] and performing a POVM with m outcomes takes time $O(m^2)$, according to the Naimark's dilation theorem that converts m -outcome POVM to projective measurement via an m -dimensional unitary gate [50] implementable with $O(m^2)$ basic gates [51]. To perform the POVM with $m = d_B^2$ elements, we need $O(d_B^4)$ gates, and thus the query part takes a total time $O(Nn(d_A + d_B^4))$. The estimation part invokes **Function 3** for n^2 times, and each call to **Function 3** takes time $O(N + d_A^4 d_B^4)$, $O(N)$ for computing \hat{p} and $O(d_A^4 d_B^4)$ for handling matrices and vectors. We don't count the time of inverting the matrix F (G) since they are known before the execution of the algorithm and their inverses can be computed in advance. To sum up, the computational complexity of **Algorithm 2** is $O(Nn(n + d_A + d_B^4) + n^2 d_A^4 d_B^4)$. If we take $N = \Omega(d_A^4 d_B^4)$, consistent with the analysis of the sample complexity in the previous paragraph, the first term dominates and the computational complexity is $O(Nn(n + d_A + d_B^4))$. \square

Supplementary Note 5 Details of the algorithm under Assumption 4

In this section, we give the pseudocode of the algorithm under Assumption 4 and the proof of its correctness (Theorem 3).

Algorithm 3: Quantum causal unravelling algorithm under Assumption 4

Input : Black-box access of a quantum comb \mathcal{C} with input wires A_1, \dots, A_n and output wires B_1, \dots, B_n ,
 number of queries N , threshold χ_-

Output : Ordering of inputs and outputs

```

1  ind  $\leftarrow$  independence( $\mathcal{C}, N, \chi_-$ );
2  Initialize Boolean arrays matchedA and matchedB to false;
3  for  $i \leftarrow 1$  to  $n$  do
4      for  $j \leftarrow 1$  to  $n$  do
5          if ind $i,j$  = false then
6               $\pi(i) \leftarrow j$ ;
7              matchedA( $i$ )  $\leftarrow$  true;
8              matchedB( $j$ )  $\leftarrow$  true;
9              break ;                               // Exit the loop for  $j$ 
10         end
11     end
12 end
13 for  $i \leftarrow 1$  to  $n$  do
14     if matchedA( $i$ ) = false then
15         for  $j \leftarrow 1$  to  $n$  do
16             if matchedB( $j$ ) = false then
17                  $\pi(i) \leftarrow j$ ;
18                 matchedA( $i$ )  $\leftarrow$  true;
19                 matchedB( $j$ )  $\leftarrow$  true;
20                 break ;                               // Exit the loop for  $j$ 
21             end
22         end
23     end
24 end
25 Output ( $A_1, B_{\pi(1)}, \dots, A_n, B_{\pi(n)}$ );

```

Algorithm 3 first matches the pairs (A_i, B_j) that are correlated, and according to Assumption 4, A_i and B_j must belong to the same tooth. For the inputs and outputs left unmatched by the first step, they can be matched arbitrarily,

since the inputs and outputs have no correlation and are compatible with any causal unravelling.

If we further assume that for each correlated input-output pair (A_i, B_j) , one has $\chi_1(A_i; B_j)_\rho \geq \chi_{\min}$ for some $\chi_{\min} > 0$, then [Algorithm 3](#) produces an exact answer $(\mathcal{C} \in \text{Comb}[(A_1, B_{\pi(1)}), \dots, (A_n, B_{\pi(n)})])$ if one take $\chi_- = \chi_{\min}/3$, and the sample complexity is given by Eq. (2). On the other hand, if such assumption of χ_{\min} does not exist, the algorithm still produces an answer, which is approximate.

Here we consider the case where no assumption on χ_{\min} is made, and give the correctness and efficiency ([Theorem 3](#)) merely based on [Assumption 4](#).

Proof of Theorem 3. Picking $\chi_- = \varepsilon_0$, according to [Lemma 7](#), with probability $1 - n^2 \kappa_0$,

1. if $\text{ind}_{i,j} = \text{false}$, then $\chi_1(A_i; B_j)_C > 0$
2. if $\text{ind}_{i,j} = \text{true}$, then $\chi_1(A_i; B_j)_C \leq 2\chi_-$

Since by [Assumption 4](#), for every input A_i , there is at most one output B_j such that $\chi_1(A_i; B_j)_C > 0$, and therefore there is at most one j satisfying $\text{ind}_{i,j} = \text{false}$. Let $A_{\text{matched}} := \{A_i | \exists j, \text{ind}_{i,j} = \text{false}\}$ and $B_{\text{matched}} := \{B_{\pi(i)} | A_i \in A_{\text{matched}}\}$ be the inputs and outputs that are matched up to [line 12](#) of [Algorithm 3](#).

Define the channel \mathcal{D} by its action on product states as follows:

$$\mathcal{D}(\rho_{A_1} \otimes \dots \otimes \rho_{A_n}) := \bigotimes_{i \in A_{\text{matched}}} \mathcal{C}_{A_i \rightarrow B_{\pi(i)}}(\rho_{A_i}) \otimes \bigotimes_{i \notin A_{\text{matched}}} \mathcal{C}_{A_i \rightarrow B_{\pi(i)}}(\rho_{A_i}) \quad (47)$$

where $\mathcal{C}_{A_i \rightarrow B_{\pi(i)}}(\rho_{A_i}) := \text{Tr}_{B_{\neq \pi(i)}}[\mathcal{C}(\rho_{A_i} \otimes I_{A_{\neq i}}/d_{A_{\neq i}})]$ is channel \mathcal{C} restricted on input A_i and output $B_{\pi(i)}$, and $\mathcal{C}_{A_i \rightarrow B_{\pi(i)}}(\rho_{A_i}) := \text{Tr}[\rho_{A_i}]C_{B_{\pi(i)}}$ is a constant channel that outputs $C_{B_{\pi(i)}}$, the marginal Choi state of \mathcal{C} on system $B_{\pi(i)}$.

Clearly, $\mathcal{D} \in \text{Comb}[(A_1, B_{\pi(1)}), \dots, (A_n, B_{\pi(n)})]$, since it is a tensor product of channels from A_i to $B_{\pi(i)}$. Now we show that the difference between \mathcal{C} and \mathcal{D} is small.

According to [Assumption 4](#), $\mathcal{C} = \bigotimes_{i=1}^n \mathcal{C}_{A_i \rightarrow B_{\pi'(i)}} = \bigotimes_{i \in A_{\text{matched}}} \mathcal{C}_{A_i \rightarrow B_{\pi'(i)}} \otimes \bigotimes_{i \notin A_{\text{matched}}} \mathcal{C}_{A_i \rightarrow B_{\pi'(i)}}$. For channel \mathcal{C} and each $i \in A_{\text{matched}}$, A_i is correlated to $B_{\pi(i)}$ but not correlated to all other outputs, and by the way π is computed, one must have $\pi(i) = \pi'(i)$. Therefore,

$$\|\mathcal{C} - \mathcal{D}\|_\diamond = \left\| \bigotimes_{i \in A_{\text{matched}}} \mathcal{C}_{A_i \rightarrow B_{\pi'(i)}} \otimes \bigotimes_{i \notin A_{\text{matched}}} \mathcal{C}_{A_i \rightarrow B_{\pi'(i)}} - \bigotimes_{i \in A_{\text{matched}}} \mathcal{C}_{A_i \rightarrow B_{\pi(i)}} \otimes \bigotimes_{i \notin A_{\text{matched}}} \mathcal{C}_{A_i \rightarrow B_{\pi(i)}} \right\|_\diamond \quad (48)$$

$$= \left\| \bigotimes_{i \notin A_{\text{matched}}} \mathcal{C}_{A_i \rightarrow B_{\pi'(i)}} - \bigotimes_{i \notin A_{\text{matched}}} \mathcal{C}_{A_i \rightarrow B_{\pi(i)}} \right\|_\diamond \quad (49)$$

and the difference between \mathcal{C} and \mathcal{D} only occurs in the second part involving $i \notin A_{\text{matched}}$. Since

$$\bigotimes_{i \notin A_{\text{matched}}} \text{Tr}[\rho_{A_i}]C_{B_{\pi(i)}} = \prod_{i \notin A_{\text{matched}}} \text{Tr}[\rho_{A_i}] \bigotimes_{j \notin B_{\text{matched}}} C_{B_j} = \bigotimes_{i \notin A_{\text{matched}}} \text{Tr}[\rho_{A_i}]C_{B_{\pi'(i)}} \quad (50)$$

we have $\bigotimes_{i \notin A_{\text{matched}}} \mathcal{C}_{A_i \rightarrow B_{\pi(i)}} = \bigotimes_{i \notin A_{\text{matched}}} \mathcal{C}_{A_i \rightarrow B_{\pi'(i)}}$, where $\mathcal{C}_{A_i \rightarrow B_{\pi'(i)}}$ is the constant channel defined as $\mathcal{C}_{A_i \rightarrow B_{\pi'(i)}}(\rho_{A_i}) := \text{Tr}[\rho_{A_i}] \mathcal{C}_{B_{\pi'(i)}}$. Eq. (49) then becomes

$$\|\mathcal{C} - \mathcal{D}\|_{\diamond} = \left\| \bigotimes_{i \notin A_{\text{matched}}} \mathcal{C}_{A_i \rightarrow B_{\pi'(i)}} - \bigotimes_{i \notin A_{\text{matched}}} \mathcal{C}_{A_i \rightarrow B_{\pi'(i)}} \right\|_{\diamond} \leq \sum_{i \notin A_{\text{matched}}} \|\mathcal{C}_{A_i \rightarrow B_{\pi'(i)}} - \mathcal{C}_{A_i \rightarrow B_{\pi'(i)}}\|_{\diamond} \quad (51)$$

Consider the channel $\mathcal{C}_{A_i \rightarrow B_{\pi'(i)}}$. For $i \notin A_{\text{matched}}$, $\text{ind}_{i, \pi'(i)} = \text{true}$ and with high probability $\chi_1(A_i; B_{\pi'(i)})_C \leq 2\chi_-$. By definition of χ_1 ,

$$\|C_{A_i, B_{\pi'(i)}} - C_{A_i} \otimes C_{B_{\pi'(i)}}\|_1 = \left\| C_{A_i, B_{\pi'(i)}} - \frac{I_{A_i}}{d_{A_i}} \otimes C_{B_{\pi'(i)}} \right\|_1 \leq 2\chi_- \quad (52)$$

Eq. (52) is the distance between the Choi states of $\mathcal{C}_{A_i \rightarrow B_{\pi'(i)}}$ and $\mathcal{C}_{A_i \rightarrow B_{\pi'(i)}}$, which gives a bound of the diamond-norm distance between the channels:

$$\|\mathcal{C}_{A_i \rightarrow B_{\pi'(i)}} - \mathcal{C}_{A_i \rightarrow B_{\pi'(i)}}\|_{\diamond} \leq d_{A_i} \left\| C_{A_i, B_{\pi'(i)}} - \frac{I_{A_i}}{d_{A_i}} \otimes C_{B_{\pi'(i)}} \right\|_1 \leq 2d_{A_i} \chi_- \quad (53)$$

Combining Eqs. (51) and (53), we obtain

$$\|\mathcal{C} - \mathcal{D}\|_{\diamond} \leq 2\chi_- \sum_{i \notin A_{\text{matched}}} d_{A_i} \leq 2nd_A \varepsilon_0 \quad (54)$$

where $d_A := \max_i d_{A_i}$. The sample complexity of [Algorithm 3](#) is given by [Lemma 2](#) as

$$N = O(d_A^6 d_B^6 \varepsilon_0^{-2} \log(d_A d_B \kappa_0^{-1})) \quad (55)$$

Let $\kappa := n^2 \kappa_0$ and $\varepsilon := 2nd_A \varepsilon_0$, we have

$$N = O(n^2 d_A^8 d_B^6 \varepsilon^{-2} \log(nd_A d_B \kappa^{-1})) \quad (56)$$

and with probability $1 - \kappa$, $\|\mathcal{C} - \mathcal{D}\|_{\diamond} \leq \varepsilon$. The running time of [Algorithm 3](#) is the same as [Algorithm 2](#) and has been discussed in [Supplementary Note 4](#). \square

Supplementary Note 6 Analysis of the causal unravelling algorithm in the approximate case

We first define the ‘approximate rank’ of a state to characterize the lowest-rank state close to a given state with respect to the Hilbert-Schmidt distance.

Definition 3.

$$\text{rank}_\eta(\rho) := \min_{\sigma: \|\sigma - \rho\|_2 \leq \eta} \text{rank}(\sigma) \quad (57)$$

Using rank_η , we write down the assumption for approximate causal unravelling, bounding the approximate ranks of marginal Choi state of \mathcal{C} .

Assumption 5. Let the output of *Algorithm 1* be $(A_{\sigma(1)}, B_{\pi(1)}), \dots, (A_{\sigma(n)}, B_{\pi(n)})$. Let $\mathcal{C}^{(k, k-1)}$ be the reduced map of \mathcal{C} obtained by keeping only the first k inputs $A_{\sigma(1)}, \dots, A_{\sigma(k)}$ and $k-1$ outputs $B_{\pi(1)}, \dots, B_{\pi(k-1)}$, and let $C^{(k, k-1)}$ be the Choi state of $\mathcal{C}^{(k, k-1)}$. We assume that $C^{(k, k-1)}$ are approximately polynomial-rank, namely

$$\forall k = 2, \dots, n, \text{rank}_{\eta^{(k)}}(C^{(k, k-1)}) = r^{(k)}, \quad (58)$$

where $\eta^{(k)}$ are small non-negative numbers and $r^{(k)}$ are bounded by a polynomial of n .

Note that **Assumption 5** can be efficiently verified. Ref. [52] provides an algorithm to decide whether a state ρ is close to a low-rank state, namely whether there exists ρ' such that $\|\rho - \rho'\|_1 \leq \varepsilon$ and $\text{rank}(\rho') \leq r$, in time $\Theta(r^2 \varepsilon^{-1})$. The algorithm in Ref. [52] is for trace distance, but can be translated easily to the Hilbert-Schmidt distance via Eq. (5) to verify Eq. (58). Given this algorithm, we can verify **Assumption 5** during the execution of *Algorithm 1*. In the $(n - k + 1)$ -th recursive call, the value of \mathcal{C} entering the algorithm is $\mathcal{C}^{(k)}$, and the state $C^{(k, k-1)}$ can be obtained by $C^{(k, k-1)} = \text{Tr}_{B_y}[C^{(k)}]$, for every candidate B_y . Therefore, we can insert one extra step in the **foreach** loop to verify whether $C^{(k, k-1)}$ is close enough to a rank- $r^{(k)}$ state. In the complexity analysis, we assume **Assumption 5** is true and do not include the time to verify it.

Under **Assumption 5**, the error and efficiency of *Algorithm 1* are given in the following theorem.

Theorem 4. Under **Assumption 5**, for any confidence parameter $\kappa_0 > 0$, *Algorithm 1* outputs a causal unravelling $(A_1, B_{\pi(1)}), \dots, (A_n, B_{\pi(n)})$ satisfying the following conditions:

1. With probability $1 - \kappa_0$, the output of *Algorithm 1* is an approximate causal unravelling for \mathcal{C} in the following sense:

$$\exists \mathcal{D} \in \text{Comb}[(A_{\sigma(1)}, B_{\pi(1)}), \dots, (A_{\sigma(n)}, B_{\pi(n)})], \|C - \mathcal{D}\|_1 \leq 8\sqrt{2} n r_{\max}^{1/4} \eta_{\max}^{1/2}, \quad (59)$$

where $\eta_{\max} := \max_k \{\eta^{(k)}\}$ and $r_{\max} := \max_k \{r^{(k)}\}$.

2. The number of queries to \mathcal{C} is in the order of

$$T_{\text{sample}} = O(n^3 \eta_{\max}^{-4} \log(n \kappa_0^{-1})). \quad (60)$$

3. The computational complexity is in the order of $O(T_{\text{sample}} n \log d_A)$.

We prove [Theorem 4](#) in the following subsections. In [Supplementary Note 6 a](#), we analyze the accuracy of the independence tests in the approximate case. In [Supplementary Note 6 b](#) we analyze how the error in each recursion step affects the final error of the algorithm. The main proof of [Theorem 4](#) is in [Supplementary Note 6 c](#).

a. Accuracy of independence tests

The following lemma is useful for converting the Hilbert-Schmidt distance to the trace distance in the approximate case.

Lemma 9. For two quantum states ρ and σ ,

$$\|\rho - \sigma\|_1 \leq \sqrt{4\text{rank}_\eta(\sigma)} (\|\rho - \sigma\|_2 + 2\eta) \quad (61)$$

Proof. By definition of rank_η , there exists a state σ' such that $\text{rank}(\sigma') = \text{rank}_\eta(\sigma)$ and $\|\sigma - \sigma'\|_2 \leq \eta$. By Eq. (5), $\|\rho - \sigma'\|_1 \leq \sqrt{4\text{rank}(\sigma')} \|\rho - \sigma'\|_2$, and we have

$$\|\rho - \sigma\|_1 \leq \|\rho - \sigma'\|_1 + \|\sigma - \sigma'\|_1 \quad (62)$$

$$\leq \sqrt{4\text{rank}(\sigma')} \|\rho - \sigma'\|_2 + \sqrt{4\text{rank}(\sigma')} \|\sigma - \sigma'\|_2 \quad (63)$$

$$\leq \sqrt{4\text{rank}(\sigma')} (\|\rho - \sigma\|_2 + \|\sigma - \sigma'\|_2) + \sqrt{4\text{rank}(\sigma')} \|\sigma - \sigma'\|_2 \quad (64)$$

$$\leq \sqrt{4\text{rank}(\sigma')} (\|\rho - \sigma\|_2 + 2\|\sigma - \sigma'\|_2) \quad (65)$$

$$= \sqrt{4\text{rank}_\eta(\sigma)} (\|\rho - \sigma\|_2 + 2\eta) \quad (66)$$

□

We first consider the accuracy of the independence test implemented in [Function 2](#), in an arbitrary iteration of [Algorithm 1](#). Define $C_1 := \text{Tr}_{B_y}[C]$ and $C_2 := I_{A_x}/d_{A_x} \otimes \text{Tr}_{A_x B_y}[C]$ as in [Function 2](#). By [Lemma 1](#), for each of the estimate p_i , ($i = 1, 2, 3$), with probability $1 - \kappa$, p_i is ε -close to the true value. By the union bound, with probability at least $1 - 3\kappa$, all three estimates are ε -close to their corresponding true values, and therefore

$$\begin{aligned} & |p_1 + p_2 - 2p_3 - \|C_1 - C_2\|_2^2| \\ & \leq |p_1 - \text{Tr}[C_1^2]| + |p_2 - \text{Tr}[C_2^2]| + |2p_3 - 2\text{Tr}[C_1 C_2]| \\ & \leq 4\varepsilon. \end{aligned} \quad (67)$$

Next, by [Lemma 9](#) and Eq. (5),

$$\sqrt{2}\|C_1 - C_2\|_2 \leq \|C_1 - C_2\|_1 \leq \sqrt{4\text{rank}_\eta(C_1)} (\|C_1 - C_2\|_2 + 2\eta) \quad (68)$$

Now we consider the output of **Function 2**. If **Function 2** returns **true**, then $p_1 + p_2 - 2p_3 \leq \delta$. From Eq. (67), $\|C_1 - C_2\|_2 \leq \sqrt{\delta + 4\varepsilon}$ and then from Eq. (68), $\|C_1 - C_2\|_1 \leq \sqrt{4\text{rank}_\eta(C_1)} (\|C_1 - C_2\|_2 + 2\eta) \leq \sqrt{4\text{rank}_\eta(C_1)} (\sqrt{\delta + 4\varepsilon} + 2\eta)$. Since $\chi_1(A_x; A_{\neq x} B_{\neq y})_C = \|C_1 - C_2\|_1$, we have the following lemma:

Lemma 10. *Let C be the input channel of **Function 2**. With probability $1 - 3\kappa$, **Function 2** satisfies the following:*

1. If **Function 2** returns **true**, then

$$\chi_1(A_x; A_{\neq x} B_{\neq y})_C \leq \sqrt{4\text{rank}_\eta(\text{Tr}_{B_y}[C])} (\sqrt{\delta + 4\varepsilon} + 2\eta), \quad (69)$$

where C is the Choi state of C ;

2. If **Function 2** returns **false**, then

$$\chi_1(A_x; A_{\neq x} B_{\neq y})_C > \sqrt{2(\delta - 4\varepsilon)}. \quad (70)$$

b. Combining errors in all recursions

Lemma 11. *For quantum states ρ and σ in Hilbert space \mathcal{H}_A , if $\|\rho - \sigma\|_1 \leq \varepsilon$, then for any purification of ρ , $|\psi\rangle_{AR}$ with an ancillary system R satisfying $\dim R \geq \text{rank}(\sigma)$, there exists a purification of σ , $|\phi\rangle_{AR}$ such that*

$$\| |\psi\rangle\langle\psi| - |\phi\rangle\langle\phi| \|_1 \leq 2\sqrt{\varepsilon} \quad (71)$$

Proof. By Uhlmann's Theorem, there exists a purification of σ , $|\phi\rangle_{AR}$ such that $F(\rho, \sigma) = F(|\psi\rangle\langle\psi|, |\phi\rangle\langle\phi|)$.

$$\frac{1}{2} \| |\psi\rangle\langle\psi| - |\phi\rangle\langle\phi| \|_1 = \sqrt{1 - F(|\psi\rangle\langle\psi|, |\phi\rangle\langle\phi|)} = \sqrt{1 - F(\rho, \sigma)} \leq \sqrt{1 - \left(1 - \frac{1}{2}\|\rho - \sigma\|_1\right)^2} \leq \sqrt{\varepsilon - \varepsilon^2/4} \leq \sqrt{\varepsilon} \quad (72)$$

□

Lemma 12. *Let C be a quantum channel and C be its Choi state. Let $C^{(i)} := \text{Tr}_{A_{i+1}B_{i+1}\dots A_n B_n}[C]$ be the Choi operator on first i input-output pairs. For $n \geq 2$, if*

$$\forall i = 2, \dots, n, \exists \mathcal{D}^{(i)\circ} \in \text{Comb}[(A_1 \dots A_{i-1}, B_1 \dots B_{i-1}), (A_i, \emptyset)], \|C^{(i)\circ} - D^{(i)\circ}\|_1 \leq \delta^{(i)}, \quad (73)$$

(Note that the above can be directly obtained from $\chi_1(A_i; A_1 \dots A_{i-1} B_1 \dots B_{i-1})_C \leq \delta^{(i)}$.) where $C^{(i)\circ} := \text{Tr}_{B_i}[C^{(i)}]$,

then

$$\exists \mathcal{D} \in \text{Comb}[(A_1, B_1), \dots, (A_n, B_n)], \quad \|C - D\|_1 \leq 2\sqrt{\delta^{(2)}} + 4 \sum_{i=3}^n \sqrt{\delta^{(i)}}, \quad (74)$$

where D is the Choi state of \mathcal{D} .

Proof.

In this proof, calligraphic letters denote linear maps and italic letters denote the corresponding Choi states.

Define a proposition $P(i)$: there exists a purification of $C^{(i)}$, denoted as $C^{(i)*} \in S(\mathcal{H}_{A_1 \dots A_i} \otimes \mathcal{H}_{B_1 \dots B_i} \otimes \mathcal{H}_{M_i})$, where M_i is the purifying system, and an isometric channel $\mathcal{E}^{(i)*} \in \text{Comb}[(A_1, B_1), \dots, (A_{i-1}, B_{i-1}), (A_i, B_i M_i)]$ such that

$$\|C^{(i)*} - E^{(i)*}\|_1 \leq \varepsilon^{(i)}. \quad (75)$$

Consider $P(2)$. Pick any purification of $C^{(2)}$ as $C^{(2)*}$, and $C^{(2)*}$ is also a purification of $C^{(2)\circ}$. Pick a purification of $D^{(2)\circ}$ as $D^{(2)*}$ such that its trace distance to $C^{(2)*}$ is minimized. Since $\|C^{(2)\circ} - D^{(2)\circ}\|_1 \leq \delta^{(2)}$, according to **Lemma 11**, we have $\|C^{(2)*} - D^{(2)*}\|_1 \leq 2\sqrt{\delta^{(2)}}$. By choosing $E^{(2)*} = D^{(2)*}$, we prove $P(2)$ with $\varepsilon^{(2)} = 2\sqrt{\delta^{(2)}}$.

Assume $P(i-1)$ holds with $\varepsilon^{(i-1)}$, then there exists a purification of $C^{(i-1)}$, denoted as $C^{(i-1)*} \in S(\mathcal{H}_{A_1 \dots A_{i-1}} \otimes \mathcal{H}_{B_1 \dots B_{i-1}} \otimes \mathcal{H}_{M_{i-1}})$, and an isometric channel $\mathcal{E}^{(i-1)*} \in \text{Comb}[(A_1, B_1), \dots, (A_{i-2}, B_{i-2}), (A_{i-1}, B_{i-1} M_{i-1})]$ such that

$$\|C^{(i-1)*} - E^{(i-1)*}\|_1 \leq \varepsilon^{(i-1)}. \quad (76)$$

Pick a purification of $C^{(i)}$ as $C^{(i)*} \in S(\mathcal{H}_{A_1 \dots A_i} \otimes \mathcal{H}_{B_1 \dots B_i} \otimes \mathcal{H}_{M_i})$ where \mathcal{H}_{M_i} is a large enough Hilbert space. Then $C^{(i)*}$ is also a purification of $C^{(i)\circ}$. Pick a purification of $D^{(i)\circ}$ as $D^{(i)*}$ such that its trace distance to $C^{(i)*}$ is minimized. Since $\|C^{(i)\circ} - D^{(i)\circ}\|_1 \leq \delta^{(i)}$ (73), according to **Lemma 11**, we have

$$\|C^{(i)*} - D^{(i)*}\|_1 \leq 2\sqrt{\|C^{(i)\circ} - D^{(i)\circ}\|_1} \leq 2\sqrt{\delta^{(i)}}. \quad (77)$$

Let $(D')^{(i-1)} := \text{Tr}_{A_i}[D^{(i)\circ}]$. Pick a purification of $(D')^{(i-1)}$ as $(D')^{(i-1)*} \in S(\mathcal{H}_{A_1 \dots A_{i-1}} \otimes \mathcal{H}_{B_1 \dots B_{i-1}} \otimes \mathcal{H}_{M_{i-1}})$ such that its trace distance to $C^{(i-1)*}$ is minimized. From **Lemma 11** we have

$$\|(D')^{(i-1)*} - C^{(i-1)*}\|_1 \leq 2\sqrt{\|(D')^{(i-1)} - C^{(i-1)}\|_1} = 2\sqrt{\|\text{Tr}_{A_i}[D^{(i)\circ} - C^{(i)\circ}]\|_1} \leq 2\sqrt{\|D^{(i)\circ} - C^{(i)\circ}\|_1} \leq 2\sqrt{\delta^{(i)}} \quad (78)$$

Note that $\mathcal{D}^{(i)*} \in \text{Comb}[(A_1 \dots A_{i-1}, B_1 \dots B_{i-1}), (A_i, B_i M_i)]$ since $\mathcal{D}^{(i)\circ} \in \text{Comb}[(A_1 \dots A_{i-1}, B_1 \dots B_{i-1}), (A_i, \emptyset)]$. Therefore $\mathcal{D}^{(i)*}$ can be written as a concatenation of two channels with the first channel being $(D')^{(i-1)*}$:

$$\mathcal{D}^{(i)*} = (\mathcal{I}_{B_1 \dots B_{i-1}} \otimes \mathcal{D}_i) \circ ((\mathcal{D}')^{(i-1)*} \otimes \mathcal{I}_{A_i}) \quad (79)$$

where $\mathcal{D}_i : S(\mathcal{H}_{A_i} \otimes \mathcal{H}_{M_{i-1}}) \rightarrow S(\mathcal{H}_{B_i} \otimes \mathcal{H}_{M_i})$ is an isometric channel since $\mathcal{D}^{(i)*}$ is isometric.

Define

$$\mathcal{E}^{(i)*} := (\mathcal{I}_{B_1 \dots B_{i-1}} \otimes \mathcal{D}_i) \circ (\mathcal{E}^{(i-1)*} \otimes \mathcal{I}_{A_i}) \quad (80)$$

and let $E^{(i)*}$ be its Choi state. This is an isometric channel because both \mathcal{D}_i and $\mathcal{E}^{(i-1)*}$ are. Define $\tilde{\mathcal{D}}_i(\rho) : S(\mathcal{H}_{M_{i-1}}) \rightarrow S(\mathcal{H}_{A'_i} \otimes \mathcal{H}_{B_i} \otimes \mathcal{H}_{M_i})$ as $\tilde{\mathcal{D}}_i(\rho) := (\mathcal{D}_i \otimes \mathcal{I}_{A'_i})(\rho \otimes |\Phi^+\rangle \langle \Phi^+|_{A_i A'_i})$, which is an isometric channel and preserves trace norm. Then we have

$$\begin{aligned} \|D^{(i)*} - E^{(i)*}\|_1 &= \left\| (\tilde{\mathcal{D}}_i \otimes \mathcal{I}_{A'_1 \dots A'_i} \otimes \mathcal{I}_{B_1 \dots B_{i-1}}) \left((D')^{(i-1)*} - E^{(i-1)*} \right) \right\|_1 \\ &= \|(D')^{(i-1)*} - E^{(i-1)*}\|_1 \\ &\leq \|(D')^{(i-1)*} - C^{(i-1)*}\|_1 + \|C^{(i-1)*} - E^{(i-1)*}\|_1 \\ &\leq 2\sqrt{\delta^{(i)}} + \varepsilon^{(i-1)} \end{aligned} \quad (81)$$

where the last step uses Eqs. (78) and (76).

Last, from Eqs. (77) and (81),

$$\|C^{(i)*} - E^{(i)*}\|_1 \leq \|C^{(i)*} - D^{(i)*}\|_1 + \|D^{(i)*} - E^{(i)*}\|_1 \leq 4\sqrt{\delta^{(i)}} + \varepsilon^{(i-1)} \quad (82)$$

Therefore, we can choose $\varepsilon^{(i)} = \varepsilon^{(i-1)} + 4\sqrt{\delta^{(i)}}$. Performing induction with base case $\varepsilon^{(2)} = 2\sqrt{\delta^{(2)}}$, we have

$$\varepsilon^{(n)} = 2\sqrt{\delta^{(2)}} + 4 \sum_{i=3}^n \sqrt{\delta^{(i)}} \quad (83)$$

Picking $D := \text{Tr}_{M_n}[E^{(n)*}]$, we have

$$\|C - D\|_1 \leq \|C^{(n)*} - E^{(n)*}\|_1 \leq \varepsilon^{(n)} = 2\sqrt{\delta^{(2)}} + 4 \sum_{i=3}^n \sqrt{\delta^{(i)}} \quad (84)$$

□

c. Proof of [Theorem 4](#)

Now we are ready to prove [Theorem 4](#).

Proof of Theorem 4. In Algorithm 1, using the relation $T_{\text{test}}(n) \leq n^2 + T_{\text{test}}(n-1)$, we can find that there are $T_{\text{test}}(n) \leq n^3$ independence tests, each of which invokes three SWAP tests. Each SWAP test produces an estimate within error ε with probability no less than $1 - \kappa$ according to Lemma 1. Let $\kappa = \kappa_0/3n^3$, and from now we assume all SWAP tests are within error ε , which has probability no less than $1 - 3n^3\kappa = 1 - \kappa_0$.

Let $\mathcal{C}^{(n)}$ be the initial value of \mathcal{C} in Algorithm 1, and let $\mathcal{C}^{(k)}$, which has k input wires and k output wires, be the value of \mathcal{C} in the $(n-k+1)$ -th recursive call of Algorithm 1.

Consider testing whether (A_x, B_y) is the last tooth of $\mathcal{C}^{(k)}$ with Function 2. Let S be the set of all wires of $\mathcal{C}^{(k)}$ excluding A_x and B_y . If (A_x, B_y) passes the test, namely Function 2 returns **true**, by Lemma 10,

$$\chi_1(A_x; S)_{\mathcal{C}^{(k)}} \leq \sqrt{4r^{(k)}} \left(\sqrt{\delta + 4\varepsilon} + 2\eta^{(k)} \right). \quad (85)$$

By Lemma 12, there exists $\mathcal{D} \in \text{Comb}[(A_{\sigma(1)}, B_{\pi(1)}), \dots, (A_{\sigma(n)}, B_{\pi(n)})]$ satisfying

$$\|C - D\|_1 \leq 4 \sum_{i=2}^n \sqrt{\sqrt{4r^{(k)}} \left(\sqrt{\delta + 4\varepsilon} + 2\eta^{(k)} \right)} \leq 4n \sqrt{\sqrt{4r_{\max}} \left(\sqrt{\delta + 4\varepsilon} + 2\eta_{\max} \right)}, \quad (86)$$

where $\eta_{\max} := \max_k \{\eta^{(k)}\}$ and $r_{\max} := \max_k \{r^{(k)}\}$.

Now we pick δ and ε such that $\sqrt{\delta + 4\varepsilon} = 2\eta_{\max}$ and $\delta = 4\varepsilon$, which leads to $\delta = 2\eta_{\max}^2$. Then Eq. (86) simplifies to

$$\|C - D\|_1 \leq 8\sqrt{2} nr_{\max}^{1/4} \eta_{\max}^{1/2} \quad (87)$$

According to Function 1, $N = O(\varepsilon^{-2} \log \kappa^{-1}) = O(\delta^{-2} \log(n\kappa_0^{-1})) = O(\eta_{\max}^{-4} \log(n\kappa_0^{-1}))$. The sample complexity is then

$$T_{\text{sample}} = NT_{\text{test}}(n) = O(n^3 \eta_{\max}^{-4} \log(n\kappa_0^{-1})) \quad (88)$$

and the computational complexity is $O(T_{\text{sample}} n \log d_A)$ from the realization of SWAP tests.

□

Supplementary Note 7 A quantum causal unravelling algorithm with $c \geq 1$

Here we give the generalization of [Algorithm 1](#) for larger c , which decomposes the original process into the form of [Figure 2](#) where each interaction involves at most c inputs and c outputs.

Algorithm 4: Quantum causal unravelling algorithm with $c \geq 1$

Input : Black-box access to quantum channel \mathcal{C} , upper bound c of the partition size

Output : A causal unravelling of \mathcal{C}

```

1 for  $(c_P, c_Q) \in \{1, \dots, c\} \times \{1, \dots, c\}$  do
2   foreach  $P \subset \{A_1, \dots, A_{n_{in}}\}$  with  $|P| = c_P$  and  $Q \subset \{B_1, \dots, B_{n_{out}}\}$  with  $|Q| = c_Q$  do
3     if  $(P, Q)$  is the last tooth then // Done by checking whether  $P$  and  $A_{\notin P} B_{\notin Q}$  are independent
4       Let  $\mathcal{C}_{A_{\notin P}, B_{\notin Q}}(\rho) := \text{Tr}_Q[\mathcal{C}(\rho \otimes \tau_P)]$ , where  $\tau_P$  is an arbitrary state on  $P$ ;
                                                // Remove  $P$  and  $Q$  from  $\mathcal{C}$ 
5       Recursively run this algorithm on the reduced channel  $\mathcal{C}_{A_{\notin P}, B_{\notin Q}}$ ;
6       Output  $(P, Q)$  and exit this function; // Append  $(P, Q)$  to the end of the output
7     end
8   end
9 end

// The algorithm reaches here in two cases:
// 1. The channel  $\mathcal{C}$  has no input wires or no output wires, in which case the foreach-loop
//    is skipped; or
// 2. The channel  $\mathcal{C}$  cannot be further decomposed by picking no more than  $c$  inputs and
//    outputs
10 Let  $P$  be the set of input wires and  $Q$  be the set of output wires;
11 Output  $(P, Q)$  and exit this function;

```

The order that c_P and c_Q are enumerated is not explicit from the description above, but it is recommended to give priority to smaller values of c_P and c_Q . This ensures that the algorithm exhausts all possibilities for smaller partition sizes before considering larger partitions, and will output the causal unravelling with minimal partition size. This is preferred since smaller partition sizes unravels more causal information about the channel.

We analyze the complexity of [Algorithm 4](#) based on the following assumption similar to [Assumption 5](#).

Assumption 6. Let the output of [Algorithm 4](#) be $(P_1, Q_1), \dots, (P_m, Q_m)$. Let $\mathcal{C}^{(k, k-1)}$ be the reduced map of \mathcal{C} obtained by keeping only the first k partitions of inputs $P_1 \cup \dots \cup P_k$ and $k-1$ partitions of outputs $Q_1 \cup \dots \cup Q_{k-1}$, and let $C^{(k, k-1)}$ be the Choi state of $\mathcal{C}^{(k, k-1)}$. We assume that $C^{(k, k-1)}$ are approximately polynomial-rank, namely

$$\forall k = 2, \dots, m, \text{rank}_{\eta^{(k)}}(C^{(k, k-1)}) = r^{(k)}, \quad (89)$$

where $\eta^{(k)}$ are small non-negative numbers and $r^{(k)}$ are bounded by a polynomial of n .

The complexity of [Algorithm 4](#) is given in the following theorem:

Theorem 5. Under [Assumption 6](#), for any confidence parameter $\kappa_0 > 0$, [Algorithm 4](#) outputs a causal unravelling $(P_1, Q_1), \dots, (P_m, Q_m)$ satisfying the following conditions:

1. With probability $1 - \kappa_0$, the output of [Algorithm 4](#) is an approximate causal unravelling for \mathcal{C} in the following sense:

$$\exists \mathcal{D} \in \text{Comb}[(P_1, Q_1), \dots, (P_m, Q_m)], \|C - D\|_1 \leq 8\sqrt{2} m r_{\max}^{1/4} \eta_{\max}^{1/2}, \quad (90)$$

where $\eta_{\max} := \max_k \{\eta^{(k)}\}$ and $r_{\max} := \max_k \{r^{(k)}\}$.

2. The number of queries to \mathcal{C} is in the order of

$$T_{\text{sample}} = O(n^{2c+1} \eta_{\max}^{-4} \log(n \kappa_0^{-1})) \quad (91)$$

where $n = \max\{n_{\text{in}}, n_{\text{out}}\}$.

3. The computational complexity is in the order of $O(T_{\text{sample}} n \log d_A)$.

Proof. We first count the number of independence tests in [Algorithm 4](#). Let $T_{\text{test}}(n)$ be the number of independence tests required for a channel with $n_{\text{in}} \leq n$ input wires and $n_{\text{out}} \leq n$ output wires. The number of possibilities to choose from n wires a subset of no more than c wires is $\sum_{k=1}^c \binom{n}{k} = O(n^c)$. In the worst case, we need to enumerate all such subsets of input and output wires, which takes time $O(n^{2c})$. In each recursion, the number of inputs and outputs of the channel is reduced by at least one, so we obtain the recursive relation $T_{\text{test}}(n) \leq O(n^{2c}) + T_{\text{test}}(n-1)$ with $T_{\text{test}}(0) = O(1)$, solving which gives $T_{\text{test}}(n) = O(n^{2c+1})$.

The remaining part of this proof is similar to the proof of [Theorem 4](#) in [Supplementary Note 6 c](#).

Let $\mathcal{C}^{(n)}$ be the initial value of \mathcal{C} in [Algorithm 1](#), and let $\mathcal{C}^{(k)}$, which has k partitions of inputs $P_1 \cup \dots \cup P_k$ and k partitions of outputs $Q_1 \cup \dots \cup Q_k$, be the value of \mathcal{C} in the $(m-k+1)$ -th recursive call of [Algorithm 1](#).

Consider testing whether (P, Q) is the last tooth of $\mathcal{C}^{(k)}$ with [Function 2](#). Let S be the set of all wires of $\mathcal{C}^{(k)}$ excluding P and Q . If (P, Q) passes the test, namely [Function 2](#) returns **true**, by [Lemma 10](#),

$$\chi_1(P; S)_{\mathcal{C}^{(k)}} \leq \sqrt{4r^{(k)}} \left(\sqrt{\delta + 4\varepsilon} + 2\eta^{(k)} \right). \quad (92)$$

By a slight variation of [Lemma 12](#), where the premise and conclusion are defined for the newly defined $\mathcal{C}^{(k)}$ in this proof, there exists $\mathcal{D} \in \text{Comb}[(P_1, Q_1), \dots, (P_m, Q_m)]$ satisfying

$$\|C - D\|_1 \leq 4m \sqrt{\sqrt{4r_{\max}} \left(\sqrt{\delta + 4\varepsilon} + 2\eta_{\max} \right)}, \quad (93)$$

where $\eta_{\max} := \max_k \{\eta^{(k)}\}$ and $r_{\max} := \max_k \{r^{(k)}\}$. Note that the induction in the proof of [Lemma 12](#) now has m steps instead of n .

Now we pick δ and ε such that $\sqrt{\delta + 4\varepsilon} = 2\eta_{\max}$ and $\delta = 4\varepsilon$, which leads to $\delta = 2\eta_{\max}^2$. Then Eq. [\(93\)](#) simplifies to

$$\|C - D\|_1 \leq 8\sqrt{2} nr_{\max}^{1/4} \eta_{\max}^{1/2} \quad (94)$$

According to [Function 1](#), $N = O(\varepsilon^{-2} \log \kappa^{-1}) = O(\delta^{-2} \log(n\kappa_0^{-1})) = O(\eta_{\max}^{-4} \log(n\kappa_0^{-1}))$. The sample complexity is then

$$T_{\text{sample}} = NT_{\text{test}}(n) = O(n^3 \eta_{\max}^{-4} \log(n\kappa_0^{-1})) \quad (95)$$

and the computational complexity is $O(T_{\text{sample}} n \log d_A)$ from the realization of SWAP tests.

□